The Plant Cell, Vol. 19: 2636–2652, August 2007, www.plantcell.org

The Organization of High-Affinity Ammonium Uptake in *Arabidopsis* Roots Depends on the Spatial Arrangement and Biochemical Properties of AMT1-Type Transporters [W]

Lixing Yuan,[a] Dominique Loqué,[a] Soichi Kojima,[a] Sabine Rauch,[a] Keiki Ishiyama,[b] Eri Inoue,[b] Hideki Takahashi,[b] and Nicolaus von Wirén[a,1]

[a] Molecular Plant Nutrition, Institute of Plant Nutrition, University of Hohenheim, D-70593 Stuttgart, Germany
[b] RIKEN Plant Science Center, Yokohama 230-0045, Japan

The *AMMONIUM TRANSPORTER* (*AMT*) family comprises six isoforms in *Arabidopsis thaliana*. Here, we describe the complete functional organization of root-expressed AMTs for high-affinity ammonium uptake. High-affinity influx of ^{15}N-labeled ammonium in two transposon-tagged *amt1;2* lines was reduced by 18 to 26% compared with wild-type plants. Enrichment of the AMT1;2 protein in the plasma membrane and localization of *AMT1;2* promoter activity in the endodermis and root cortex indicated that AMT1;2 mediates the uptake of ammonium entering the root via the apoplasmic transport route. An *amt1;1 amt1;2 amt1;3 amt2;1* quadruple mutant (*qko*) showed severe growth depression under ammonium supply and maintained only 5 to 10% of wild-type high-affinity ammonium uptake capacity. Transcriptional upregulation of *AMT1;5* in nitrogen-deficient rhizodermal and root hair cells and the ability of *AMT1;5* to transport ammonium in yeast suggested that AMT1;5 accounts for the remaining uptake capacity in *qko*. Triple and quadruple *amt* insertion lines revealed in vivo ammonium substrate affinities of 50, 234, 61, and 4.5 μM for AMT1;1, AMT1;2, AMT1;3, and AMT1;5, respectively, but no ammonium influx activity for AMT2;1. These data suggest that two principle means of achieving effective ammonium uptake in *Arabidopsis* roots are the spatial arrangement of AMT1-type ammonium transporters and the distribution of their transport capacities at different substrate affinities.

INTRODUCTION

In plants, transport of nutrients, water, and metabolites is mostly facilitated by families of membrane transporters. Heterologous expression, tissue and subcellular localization, and physiological analysis of mutants have contributed much to our understanding of the function of individual transporters. Knockout lines have revealed functional redundancy and specialization of transporter family members. Severe growth phenotypes have been obtained by mutating individual family members in the presence of other members that show similar expression or location patterns (Hirsch et al., 1998; Javot et al., 2003; Hirner et al., 2006; Takano et al., 2006). However, most single-gene insertion mutants from multigene families have no recognizable phenotype (Sohlenkamp et al., 2002; Hussain et al., 2004; Kataoka et al., 2004; Shin et al., 2004; Lanquar et al., 2005). The scarcity of viable transporter mutants that are defective in several genes of one transporter family has somewhat hampered the characterization of transporter functions. A deeper understanding of the principles underlying a coordinated substrate transport via multiple family members in plants requires not only a consideration of the biochemical properties, cell type–specific expression patterns, and the regulation of individual transporter homologs, but also a dissection of the physiological contribution of each member. Knowledge of the molecular and physiological basis of ammonium transport in *Arabidopsis thaliana* plants is growing and points to the involvement of multiple members in defined transport functions (Gazzarrini et al., 1999; Rawat et al., 1999; Kaiser et al., 2002; Sohlenkamp et al., 2002; Lejay et al., 2003; Loqué et al., 2006). Based on these findings, uptake of ammonium by roots would appear to be a suitable process to learn how members of protein families can coordinate transport of a substrate in planta.

In a wide range of organisms, transport of ammonium across membranes is mediated by proteins of the AMMONIUM TRANSPORTER/METHYLAMMONIUM PERMEASE/RHESUS (AMT/MEP/Rh) family (von Wirén and Merrick, 2004). Plant members of this family belong either to the AMT subfamily and permeate ammonium via NH_4^+ uniport or NH_3/H^+ cotransport (Ludewig, 2006) or to the MEP subfamily that also includes AmtB from *Escherichia coli* shown to channel NH_3 across the cell membrane (Khademi et al., 2004; Zheng et al., 2004; Javelle et al., 2005). In *Arabidopsis*, AMT2;1 is the only member of the MEP subfamily, while five homologs, AMT1;1 to AMT1;5, constitute the AMT clade (Ludewig et al., 2001). At the level of individual AMT-type transporters, several mechanisms have been shown to regulate root ammonium fluxes in response to the cellular and/or whole-plant demand for nitrogen. At the transcriptional level, AMT gene expression in *Arabidopsis* roots is generally repressed by high

[1] Address correspondence to vonwiren@uni-hohenheim.de.
The author responsible for distribution of materials integral to the findings presented in this article in accordance with the policy described in the Instructions for Authors (www.plantcell.org) is: Nicolaus von Wirén (vonwiren@uni-hohenheim.de).
[W] Online version contains Web-only data.
www.plantcell.org/cgi/doi/10.1105/tpc.107.052134

nitrogen, most likely by the internal pool of Gln, and derepressed under nitrogen deficiency or supply of sugars (Gazzarrini et al., 1999; Rawat et al., 1999; Lejay et al., 2003). The nitrogen nutrition status of plants may specifically affect transcript stability, as has been observed in *Arabidopsis* for *AMT1;1* but not for *AMT1;3* (Yuan et al., 2007). At the posttranslational level, AMT1;1 can be inactivated by C-terminal phosphorylation. Most likely, AMT1;1 assembles as a trimer and the phosphorylation signal transinhibits the two neighboring subunits, representing an example of cooperative transporter regulation (Loqué et al., 2007). The tightly controlled transport of ammonium is not only essential for maintaining the cation-anion balance and plant growth (Bloom et al., 1993; Marschner, 1995) but also for adjusting levels of phytohormones regulating leaf development (Walch-Liu et al., 2000; Rahayu et al., 2005) and for preventing overaccumulation of ammonium that may otherwise cause membrane depolarization and cellular damage (Britto and Kronzucker, 2002).

Transcriptome and RNA gel blot analyses have shown that four of the six AMT/MEP homologs in *Arabidopsis* are expressed in roots and upregulated under nitrogen deficiency (Gazzarrini et al., 1999; Sohlenkamp et al., 2002; Birnbaum et al., 2003; Schmid et al., 2005). RNA interference (RNAi)-mediated repression of *AMT2;1* provided no evidence for a contribution of AMT2;1 to overall ammonium uptake (Sohlenkamp et al., 2002), whereas influx measurements in a T-DNA insertion line showed that AMT1;1 may confer approximately one-third of the overall high-affinity transport capacity in nitrogen-deficient *Arabidopsis* roots (Kaiser et al., 2002). AMT1;3 was shown to confer also a third of the high-affinity ammonium transport capacity in roots. A double insertion mutant for *AMT1;1* and *AMT1;3* had 60 to 70% reduced transport capacity, indicating an additive contribution of these transporters under nitrogen deficiency, consistent with the observation that these proteins both localize preferentially to the plasma membrane of rhizodermal cells of the root hair zone (Loqué et al., 2006). Despite the substantial reduction in high-affinity ammonium uptake in an *amt1;1 amt1;3* double mutant and the absence of any evidence for an accompanying compensatory upregulation of AMT2;1 or AMT1;2, the double insertion line showed no recognizable growth phenotype even under purely ammonium-based nitrogen nutrition. These observations suggest that other root-expressed ammonium transporters have functions redundant to AMT1;1 or AMT1;3 in root ammonium uptake and raised the question of how individual transporters are arranged to coordinate ammonium influx into roots.

We have used reverse genetics to investigate the functional organization of ammonium transporters in *Arabidopsis*. In this and a previous study (Loqué et al., 2006), we measured ammonium influx in single T-DNA or transposon insertion lines to determine the in vivo contribution of individual AMT members to overall ammonium uptake in roots. In this study, we constructed a quadruple *amt1;1 amt1;2 amt1;3 amt2;1* insertion mutant line in which 90 to 95% of the high-affinity ammonium uptake capacity was lost. Analysis of triple insertion lines in which only one of these four AMT transporter genes was functional allowed the determination of individual transporter capacities against a background of low ammonium uptake. The results indicate that high-affinity uptake of ammonium in *Arabidopsis* roots is mostly conferred by four AMT proteins. The capacities of the individual proteins are additive and enhanced under nitrogen deficiency but may vary according to the presence of the other homologs. Furthermore, we provide evidence that the biochemical transport properties of individual AMT-type proteins in roots are suited to the respective root cell types in which they are expressed, providing a potential explanation of how specialized AMTs cooperate together to achieve effective uptake of ammonium into the plant.

RESULTS

amt1;2 Transposon Insertion Lines Have a Reduced High-Affinity Ammonium Uptake Capacity in Roots

To evaluate the contribution of AMT1;2 to ammonium uptake in roots, two lines containing independent transposon insertions in this gene were obtained from the Jonathan Jones *En/Spm* collection (Tissier et al., 1999) via the Nottingham Arabidopsis Stock Centre (NASC; http://www.nasc.nott.ac.uk). The transposons in the lines *amt1;2-1* and *amt1;2-2* were found to be inserted 983 and 1375 bp downstream of the start codon of *AMT1;2*, respectively (Figure 1A). RNA gel blot analysis using the 3′-end of *AMT1;2* as probe failed to detect any *AMT1;2* transcripts in roots of *amt1;2* homozygotes for either insertion (Figure 1B). However, a full-length *AMT1;2* open reading frame (ORF) probe detected a signal in the *amt1;2-2* mutant, suggesting expression of a truncated *AMT1;2-ORF* (see Supplemental Figure 1A online). The cDNA corresponding to this transcript was cloned from *amt1;2-2* genomic DNA consisting of a fusion between the 5′-end of the *AMT1;2-ORF* and the transposon. Its sequence revealed that the DNA fusion could be translated into a chimeric protein containing the first 458 amino acids of *AMT1;2* and a short translated part of the transposon. When the corresponding cDNA was heterologously expressed in an ammonium uptake-defective yeast mutant (*Δmep1,2,3*; Marini et al., 1997), it failed to complement the defect in ammonium uptake, indicating that the translation product was either inactive or unstable (see Supplemental Figure 1B online). To evaluate plants for the presence of AMT1;2 protein, we subjected microsomal membrane fractions from roots of hydroponically grown *Arabidopsis* to protein gel blot analysis using an antibody raised against a 15–amino acid stretch in the C terminus of AMT1;2. A specific band at ~40 kD was detected in wild-type plants, which is somewhat smaller than the calculated molecular weight of AMT1;2 (55 kD), although a faster gel migration would be consistent with the hydrophobic nature of the protein (Figure 1C). An additional specific band was detected at ~80 to 90 kD, representing a possible dimer of AMT1;2 (Ludewig et al., 2003) or a stable complex with other unknown proteins. The antibody revealed no signal for membrane protein preparations from roots of the *amt1;2-1* and *amt1;2-2* insertion lines (Figure 1C). The higher molecular weight band was then evaluated for possible variation in plants deprived of nitrogen for up to 4 d. In contrast with AMT1;1 and AMT1;3, neither the 40- nor 80-kD protein band of AMT1;2 considerably changed under nitrogen deficiency (Figure 1D), indicating that the signal ratio of these two forms is not subject to nitrogen-dependent regulation.

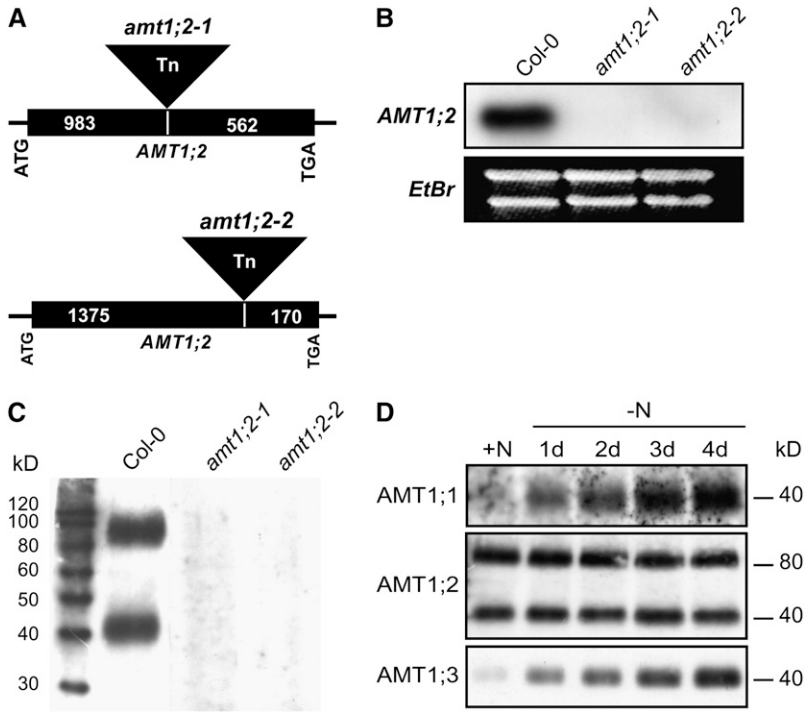

Figure 1. Characterization of Transposon Insertion Lines for *AMT1;2*.

(A) Positions of the transposon insertion sites in *AMT1;2* in the lines *amt1;2-1* and *amt1;2-2*.

(B) RNA gel blot analysis of root RNA from wild-type (Col-0), *amt1;2-1*, and *amt1;2-2* plants using the 3′-end of *AMT1;2* as a probe. Ethidium bromide–stained *rRNA* served as loading control.

(C) Protein gel blot analysis of microsomal membrane fractions from roots of wild-type (Col-0), *amt1;2-1*, and *amt1;2-2* plants using an antibody directed against 15 amino acids from the C terminus of AMT1;2. AMT1;2-specific bands were detected at ~80 and 40 kD.

(D) Protein gel blot analysis of microsomal membrane fractions from roots of 6-week-old wild-type plants (Col-0) that have been pregrown hydroponically for 1 to 4 d in the absence of nitrogen using antibodies against AMT1;1, AMT1;2, and AMT1;3.

Neither mutant line showed any visible phenotype when grown on soil or on agar medium supplemented with different concentrations of ammonium or ammonium nitrate. In the presence of methylammonium (MeA), however, both insertion lines grew slightly better than the wild type (see Supplemental Figure 2 online). At 5 to 15 mM MeA, leaves of *amt1;2-1* and *amt1;2-2* were greener and larger, suggesting a lower uptake of the toxic ammonium analog. Short-term influx of ^{15}N-labeled ammonium was determined in hydroponically grown plants precultured under different nitrogen regimes. In plants presupplied with adequate nitrogen, high-affinity ammonium uptake into the roots of both insertion lines was 28 or 23% lower than in the wild type, while in plants presupplied with insufficient nitrogen, high-affinity uptake rates decreased by 26 or 18% in *amt1;2-1* or *amt1;2-2*, respectively (Figure 2A). The mutants showed significant reductions of influx at 5 mM external substrate only after pregrowth under nitrogen deficiency (Figure 2B). However, calculation of low-affinity ammonium transport activity as the difference between influxes measured at 5 mM and 200 μM indicated that AMT1;2 did not significantly contribute to low-affinity ammonium transport activity. It was concluded that AMT1;2 represents primarily a high-affinity ammonium transporter. Gene and protein expression levels of other root-expressed AMTs in the roots of nitrogen-sufficient and -deficient plants were investigated by RNA and protein gel blot analyses. No differences in mRNA or protein levels of AMT1;1, AMT1;3, and AMT2;1 relative to the wild type were detected in the *amt1;2-1* or *amt1;2-2* mutants (Figures 2C and 2D), indicating the absence of any regulatory compensation in these three AMTs resulting from the loss of AMT1;2.

Subcellular Localization of AMT1;2

The location of AMT1;2 was investigated in membrane fractions of *Arabidopsis* roots and shoots prepared by two-phase partitioning. Enrichment of plasma membrane proteins in the upper phase was verified by protein gel blot analysis using an antibody against the plasma membrane ATPase AHA2 (DeWitt et al., 1996), while enrichment of endosomal membrane proteins in the lower fraction was confirmed by detection of DET3, a subunit of the vacuolar ATPase (Schumacher et al., 1999) and of the vacuolar pyrophosphatase (VPPase; Takasu et al., 1997). Probing of these fractions with the AMT1;2 antibody showed that in both cases, AMT1;2 was enriched in the upper phase (Figure 3). This

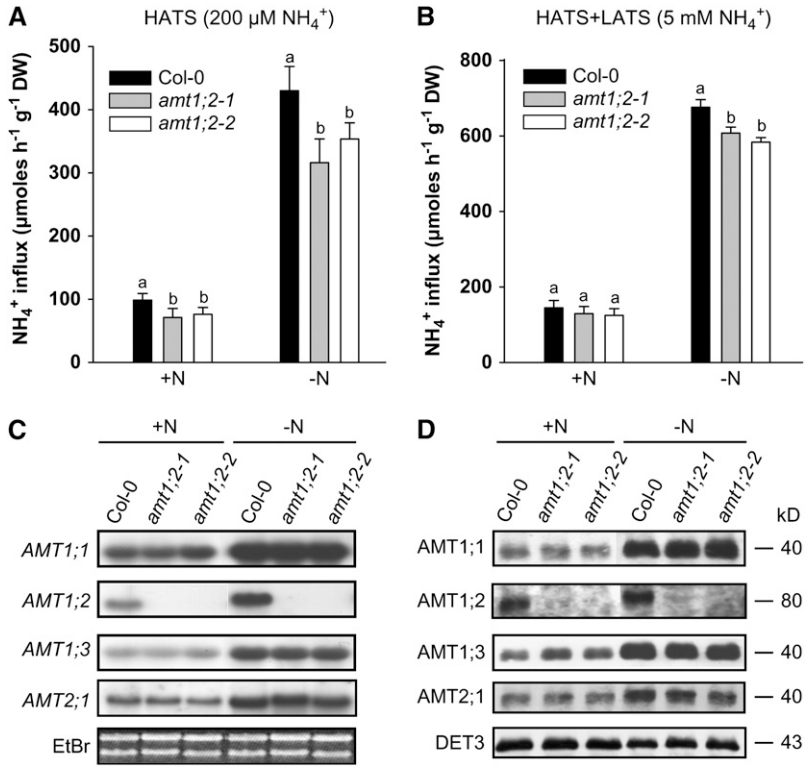

Figure 2. Ammonium Influx and Gene Expression Analysis in Roots of *amt1;2* Insertion Lines.

(A) and **(B)** Influx of ^{15}N-labeled ammonium supplied at a concentration of 200 μM being indicative for the high-affinity transport system (HATS) **(A)** or at 5 mM being indicative for the high- and low-affinity transport system (HATS+LATS) **(B)** into roots of wild-type (Col-0), *amt1;2-1*, and *amt1;2-2* plants that had been pregrown in the presence of either sufficient (+N) or insufficient (−N) nitrogen. Bars indicate means ± SD ($n = 8$ to 10 plants), and significant differences at $P < 0.001$ within each group are indicated by different letters. DW, dry weight.

(C) and **(D)** RNA gel blot analysis of root RNA **(C)** and protein gel blot analysis of microsomal membrane fractions from roots **(D)** of the same lines as in **(A)** and **(B)** using the 3′-end of *AMT1;1*, *AMT1;2*, or *AMT1;3* or the ORF of *AMT2;1* as a probe or antibodies directed against AMT1;1, AMT1;2, AMT1;3, or AMT2;1, respectively. Ethidium bromide–stained *rRNA* and protein levels of DET3 served as loading controls. Six-week-old plants were precultured hydroponically under continuous supply of 2 mM ammonium nitrate (+N) or under nitrogen deficiency for 4 d (−N).

confirmed a mainly plasma membrane location for AMT1;2 in root and shoot tissues.

Localization of AMT1;2 in Endodermis and Cortex Cells

Ammonium influx studies in single insertion lines had indicated that AMT1;2 contributes a somewhat lower absolute ammonium uptake capacity than AMT1;1 or AMT1;3 (Loqué et al., 2006). We investigated whether the tissue location of *AMT1;2* transcription could help explain the different contribution of AMT1;2. To localize AMT1;2 transcription, we examined roots of *Arabidopsis* plants expressing an *AMT1;2:green fluorescent protein* (*GFP*) fusion protein from a transgene driven by the native *AMT1;2* promoter. In plants grown in nitrogen-deficient conditions, green fluorescence was not evident in the root tip but was strong in the root hair zone and in regions further up the root (Figure 4A). In the root hair differentiation zone, longitudinal and radial sections showed the AMT1;2:GFP protein to be confined mainly to endodermal cells (Figures 4B and 4E). Higher up in the root hair zone, *AMT1;2* expression of the fusion protein also extended to cortical cells (Figures 4C and 4F), while in the zone of emerging lateral roots, GFP-dependent fluorescence became exclusively restricted to cortical cells (Figures 4D and 4G). This localization clearly differed from that of AMT1;1 and AMT1;3, which had been shown to be expressed mainly in cortical and rhizodermal cells (Loqué et al., 2006).

To investigate whether the location of AMT1;2 in inner root cells might favor root-to-shoot translocation of ammonium, xylem sap was collected from wild-type and *amt1;2* insertion lines. Ammonium concentrations in the xylem sap were in the millimolar range, confirming that this form of nitrogen is translocated in substantial amounts from roots to the shoot as in other cruciferous plant species (Finnemann and Schjoerring, 1999). A difference between wild-type and *amt1;2* insertion lines in the ammonium concentration of the xylem sap, however, was not observed, irrespective of whether plants were nitrogen deficient, resupplied with ammonium or nitrogen-sufficient, or assayed at different time points during a diurnal cycle (see Supplemental Figure 3 online).

Since AMT1;2 is expressed in inner root cell layers and its loss of function reduced ammonium uptake capacity, the lack of AMT1;2 might also reduce depletion of apoplastic ammonium

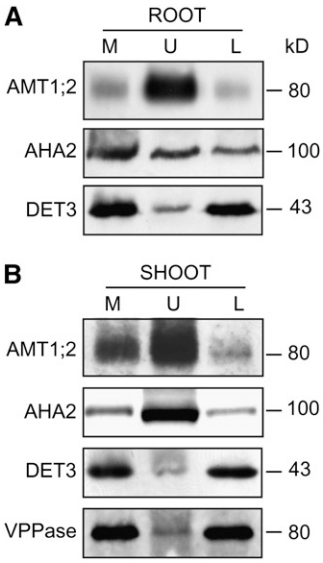

Figure 3. Subcellular Localization of AMT1;2 in *Arabidopsis*.

Microsomal fractions (M) from roots **(A)** and shoots **(B)** of nitrogen-sufficient wild-type (Col-0) plants were separated by aqueous two-phase partitioning into a plasma membrane–enriched upper phase (U) and an endosomal membrane-enriched lower phase (L). Protein gel blot analysis was conducted with antibodies against AMT1;2, an *Arabidopsis* plasma membrane H^+-ATPase (AHA2), a vacuolar H^+-ATPase subunit (DET3), and vacuolar pyrophosphatase (VPPase). Six-week-old plants were precultured hydroponically under continuous supply of 2 mM ammonium nitrate.

pools in roots. To verify this hypothesis, apoplastic fluid was extracted for ammonium analysis from wild-type and *amt1;2* plants that were nitrogen deficient or ammonium resupplied. However, no differences in apoplastic ammonium concentrations among these lines were found irrespective of whether plants were nitrogen deficient or resupplied with ammonium (Figure 5), suggesting that the size of this pool was not significantly affected by AMT1;2-mediated ammonium uptake. Unexpectedly, ammonium concentrations in the root apoplast of nitrogen-deficient plants were between 0.7 and 1 mM and increased up to 1.7 mM after resupply of 250 μM ammonium. Thus, apoplastic ammonium concentrations were several times higher than the external supply, suggesting that the apoplastic ammonium pool is maintained by the root tissue and highly buffered even under variable nitrogen regimes.

Generation of a Quadruple (*qko*) and Triple Insertion Lines

Using a double insertion mutant line, we had shown that the AMT1;1 and AMT1;3 plasma membrane–localized ammonium transporters contribute in an additive manner to high-affinity ammonium uptake in nitrogen-deficient *Arabidopsis* roots (Loqué et al., 2006). Since these AMTs, as well as AMT1;2 and AMT2;1, are all expressed in the roots (Figures 2C and 2D; Sohlenkamp et al., 2002), we made a quadruple *amt1;1-1 amt1;3-1 amt2;1-1 amt1;2-1* mutant to investigate the total contribution of these four AMTs to ammonium uptake. The source of the *amt2;1* mutant allele was the *amt2;1-1* insertion mutant line (kindly provided by Doris Rentsch, University of Bern, Switzerland, who in turn obtained it from the enhancer trap collection of Thomas Jack, Fartmouth College, NH, which was shown to contain a T-DNA insertion located 680 bp downstream of the start codon, resulting in a loss of AMT2;1 protein; see Supplemental Figure 4 online). To begin, we crossed the *amt1;1 amt1;3* double mutant with the *amt2;1-1* line and selected F2 progeny homozygous for all three mutant alleles. The *amt1;1-1 amt1;3-1 amt2;1-1* triple insertion line was then crossed to the transposon insertion line *amt1;2-1* (Figure 1) to generate a quadruple mutant *amt1;1-1 amt1;3-1 amt2;1-1 amt1;2-1* line (*qko*).

The insertion mutant alleles of the four AMT genes were derived from three different ecotype backgrounds (see Methods). To obtain lines containing individual wild-type endogenous AMT genes in a genetic background that was relatively homogeneous, we added individual wild-type AMT genes from a single ecotype back to the quadruple knockout line (*qko*) by crossing. The *qko* was crossed to wild-type Columbia (Col-0), and PCR was used to identify F3 progeny plants homozygous for insertions in three of the four AMT genes and homozygous wild type for the remaining AMT gene. The lines containing wild-type *AMT1;1*, *AMT1;2*, *AMT1;3*, or *AMT2;1* genes were named *qko+11*, *qko+12*, *qko+13*, and *qko+21*, respectively. In parallel, a homozygous *qko* line was isolated from the same F3 progeny to serve as a reference line for the triple insertion lines. Each F3 plant was allowed to self, and the F4 plants were used to conduct experiments.

Plants of these lines were cultivated in nutrient solution under nitrogen-sufficient and -deficient conditions and evaluated for expression of AMT transcript and protein. RNA and protein gel blot analyses confirmed that none of the four AMTs were detectable in *qko* and that AMT1;1, AMT1;2, AMT1;3, and AMT2;1 were expressed in the *qko+11*, *qko+12*, *qko+13*, and *qko+21* lines, respectively (Figures 6A and 6B). RNA gel blot analyses showed upregulation of wild-type *AMT1;1*, *AMT1;2*, *AMT1;3*, and *AMT2;1* transcripts under nitrogen deficiency. While protein levels of AMT1;1, AMT1;3, and possibly AMT2;1 increased under nitrogen deficiency, those of AMT1;2 did not. These results are consistent with those illustrated in Figure 1D, emphasizing little or no nitrogen-dependent regulation of AMT1;2 protein levels in *Arabidopsis* roots.

Phenotypic Analysis of *qko* and Triple Insertion Lines

When grown in a nitrate-fertilized peat-based substrate or in nutrient solution supplemented with 2 mM ammonium nitrate, neither the insertion lines nor the *qko* developed any visible phenotype. However, on sterile agar medium and in the presence of 20 or 50 mM MeA, *qko* grew dramatically better than Col-0, which was severely inhibited in root growth and shoot biomass production (Figures 7A and 7B). As expected from a lack of MeA transport activity by AMT2;1 when expressed in yeast (Sohlenkamp et al., 2000), the *qko+21* triple insertion line showed no increase in MeA sensitivity relative to the *qko*, whereas *qko+11*, *qko+12*, and *qko+13* displayed intermediate MeA sensitivities.

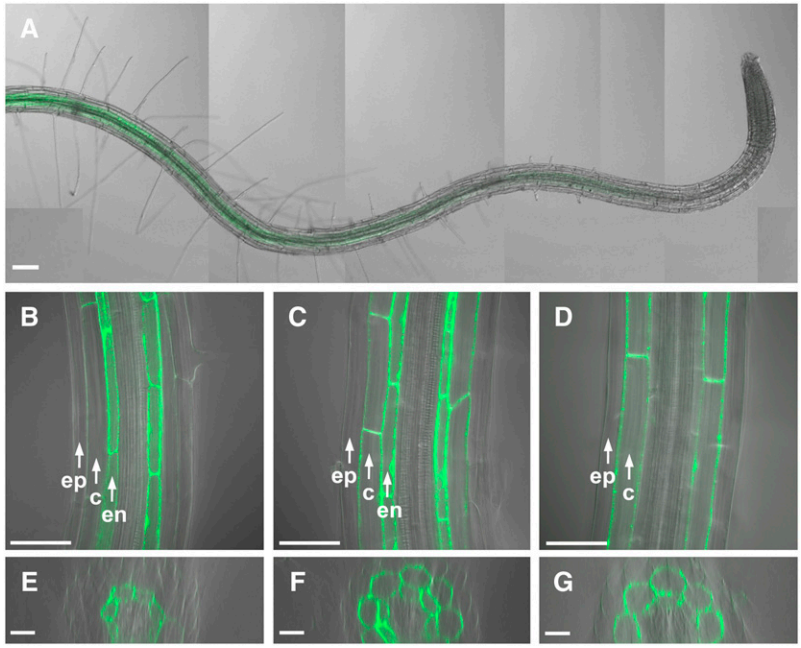

Figure 4. Localization of AMT1;2 in *Arabidopsis* Roots.

Transgenic plants expressing an *AMT1;2-promoter:ORF:GFP* fusion construct were grown on agar plates for 2 weeks.
(A) Longitudinal view of the root tip region. Bar = 100 μm.
(B) to **(D)** Longitudinal confocal sections from the root hair differentiation zone **(B)**, the mid region **(C)**, and the basal region **(D)** of the root. Bars = 50 μm.
(E) to **(G)** Cross sections from the same root zones as in **(B)** to **(D)**, respectively. The images were reconstructed from z-series of longitudinal confocal sections. ep, epidermis; co, cortex; en, endodermis. Bars = 20 μm.

Out of the *AMT1;1*, *AMT1;2*, and *AMT1;3* wild-type genes, *AMT1;2* seemed to confer the least amount of MeA sensitivity.

Phenotypes were then assessed on sterile agar medium, in which ammonium could be readily maintained as the sole nitrogen source over a few weeks. At 500 to 750 μM ammonium, on which Col-0 grew best, the *qko* produced only 50% of the shoot biomass of Col-0 (Figure 8A). Despite the lack of all four AMTs, *qko* was able to significantly increase shoot biomass at 0 to 200 μM ammonium, indicating that *qko* was still able to use ammonium supplied at low micromolar concentrations. A comparative growth analysis including the triple insertion lines on 500 μM ammonium showed that the presence of AMT1;1, AMT1;2, or AMT1;3 alone was sufficient to restore ammonium-dependent growth to the wild-type level (Figures 8B and 8C). Although shoot biomass of *qko+12* was similar to that of *qko+11* and *qko+13*, *qko+12* shoot nitrogen concentrations were lower under pure ammonium nutrition or ammonium nitrate nutrition, suggesting that AMT1;2 has a comparatively lower ammonium transport capacity. In contrast with the three AMT1 transporters, the presence of AMT2;1 in the *qko+21* triple insertion line failed to increase shoot nitrogen accumulation or biomass production relative to *qko* (Figures 8C and 8D). This failure of AMT2;1 to contribute to ammonium-based nitrogen nutrition was also reflected under supply of ammonium nitrate, in which growth of *qko+21* was repressed to similar levels as the *qko* (Figures 8B to 8D). When plants were supplied with ammonium as a sole nitrogen source at concentrations above 4 mM, growth suppression in *qko* relative to the wild type was absent, suggesting that low-affinity ammonium transport then recovered growth of *qko* (see Supplemental Figure 5 online).

Comparative Analysis of AMT Transport Properties in Planta

Short-term influx of ^{15}N-labeled ammonium into roots of *qko* and the triple insertion line at 200 μM external ammonium was examined as a measure of high-affinity transport capacity. In plants presupplied with sufficient nitrogen, ammonium influx into the roots of the *qko* or *qko+21* lines was almost ten-fold lower than in Col-0. Therefore, despite transcriptional upregulation under nitrogen deficiency, AMT2;1 was unable to contribute to short-term ammonium influx into roots. By contrast, the *qko+12* line reached 18% and the *qko+11* and *qko+13* lines reached 45 to 50% of wild-type capacity after presupply with nitrogen (Figure 9A). After pregrowth in nitrogen-deficient conditions, the *qko+11* and *qko+13* lines showed improved transport capacities of 64 and 70% of that of the wild type, respectively. However, the *qko+12* line continued to show relatively low capacity (22% of the wild type) after growth in nitrogen-deficient conditions. The lower contribution of AMT1;2 relative to AMT1;1 and AMT1;3 was in agreement with the relatively low MeA sensitivity and lower nitrogen accumulation of the *qko+12* line when grown on ammonium (Figures 7 and 8). Notably, ammonium influx in nitrogen-deficient *qko* plants increased approximately threefold to fourfold

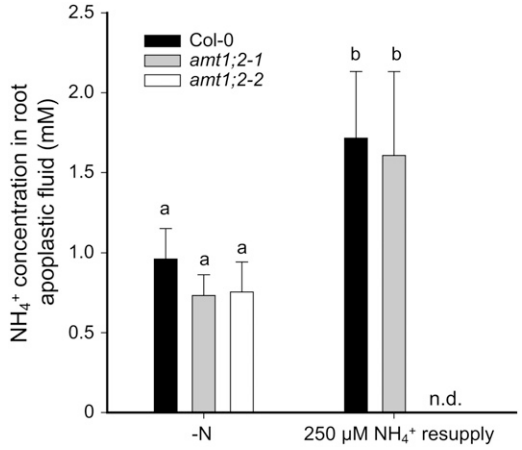

Figure 5. Ammonium Concentrations in the Apoplastic Washing Fluid from Roots.

Ammonium concentrations in the apoplastic washing fluid from roots of wild-type (Col-0) plants or roots of the insertion lines *amt1;2-1* and *amt1;2-2*. Bars indicate means ± SD ($n = 8$ to 10), and significant differences at $P < 0.05$ are indicated by different letters. Six-week-old plants were precultured hydroponically under continuous supply of 2 mM ammonium nitrate and then for 2 d under nitrogen deficiency (–N) and then resupplied with 250 μM NH_4^+ for 30 min. Root apoplasmic washing fluid was extracted by centrifugation. Determination of phosphoenol pyruvate carboxylase activity (EC4.1.1.31) indicated <1% of contamination of apoplastic washing fluid by symplastic constituents. n.d., not determined.

compared with nitrogen-sufficient plants, indicating that an unidentified nitrogen-dependent uptake system still operates in *qko*.

Nitrogen-deficient plants were subjected to a concentration-dependent ammonium influx analysis. Ammonium uptake rates in the *qko+11* and *qko+13* lines became saturated between 150 and 500 μM ammonium, with a V_{max} of 344.7 ± 14.3 and 286.6 ± 10.4 μmol h^{-1} g^{-1}, respectively, while *qko+12* only reached a capacity of 141.9 ± 11.4 μmol h^{-1} g^{-1} (Figure 9B). Reassuringly, the uptake capacities of *AMT1;2* determined by comparing the single *amt1;2* insertion lines with the wild type were in close agreement with those determined by comparing the *qko+12* triple insertion line with the *qko* line (Figures 2 and 8). Differences in uptake rates between the *qko* and triple insertion lines were direct fitted to the Michaelis-Menten equation to give estimates of in planta affinity constants for the individual ammonium transporters. These were 50.0 ± 9.6 μM for AMT1;1, 60.5 ± 13.7 μM for AMT1;3, and 233.9 ± 72.9 μM for AMT1;2.

Evidence for a Role of AMT1;5 in Residual Ammonium Influx Present in the *qko* Line

Ammonium influx in the *qko* line still increased under nitrogen deficiency. To quantify this remaining transport activity, the concentration-dependent ammonium influx into nitrogen-sufficient and -deficient *qko* plants was determined. Ammonium influx into roots of plants pregrown on adequate nitrogen followed a linear concentration dependency, while influx into nitrogen-deficient roots steeply increased between 0 and 50 μM ammonium and became saturated above 50 μM (Figure 10A). To calculate the kinetic properties of the remaining nitrogen-dependent transport system in *qko*, uptake rates determined in nitrogen-sufficient *qko* plants were subtracted from those of nitrogen-deficient plants. Plotting of the subtracted values against the external concentrations up to 500 μM ammonium did not allow the fitting of a saturation curve, while use of values up to 200 μM ammonium yielded a saturation curve with a correlation coefficient of $r^2 = 0.70$. The calculated V_{max} of the remaining nitrogen-dependent transport system in *qko* amounted to 24.3 ± 1.7 μmol h^{-1} g^{-1} at an affinity constant of 4.5 ± 1.7 μM. This indicated the existence of an as yet unidentified ammonium transport system of low capacity but very high affinity.

Prior transcriptome analyses failed to reveal expression of the two remaining AMT genes *AMT1;4* and *AMT1;5* in roots (Birnbaum et al., 2003; Schmid et al., 2005). Since these experiments were conducted with RNA from roots of wild-type plants grown in sufficient levels of nitrogen, we reexamined the expression of these two genes by quantitative RT-PCR in nitrogen-deficient roots of wild-type and *amt* mutant plants. Consistent with the previous studies, no expression of either of the two

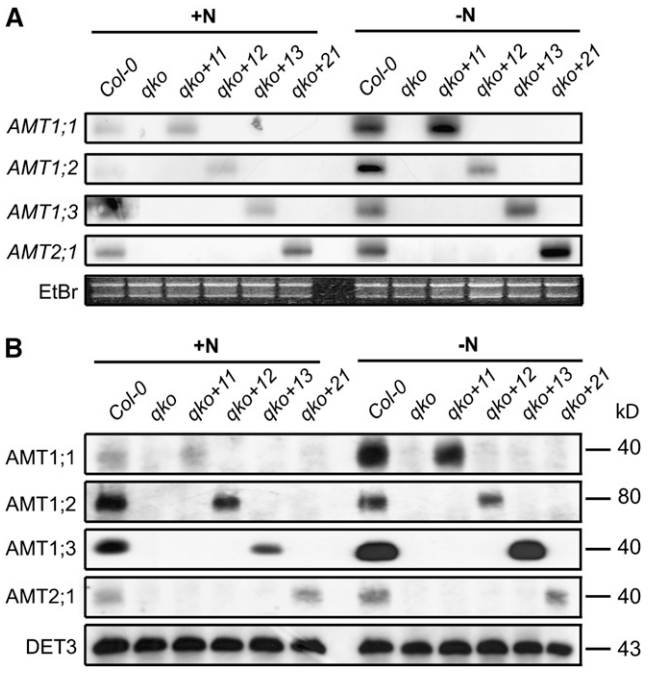

Figure 6. Characterization of a Quadruple (*qko*) and Triple Insertion Lines.

RNA gel blot analysis of root RNA **(A)** and protein gel blot analysis of microsomal membrane fractions **(B)** from roots of the wild-type (Col-0), the quadruple insertion line *qko* (*amt1;1 amt1;2 amt1;3 amt2;1*), and triple insertion lines expressing *AMT1;1* (*qko+11*), *AMT1;2* (*qko+12*), *AMT1;3* (*qko+13*), or *AMT2;1* (*qko+21*) using the 3′-ends of *AMT1;1*, *AMT1;2*, or *AMT1;3* or the ORF of *AMT2;1* as a probe or antibodies directed against AMT1;1, AMT1;2, AMT1;3, or AMT2;1, respectively. Ethidium bromide (EtBr)–stained *rRNA* and protein levels of DET3 served as loading controls. Six-week-old plants were precultured hydroponically under continuous supply of 2 mM ammonium nitrate (+N) or under nitrogen deficiency for 4 d (−N).

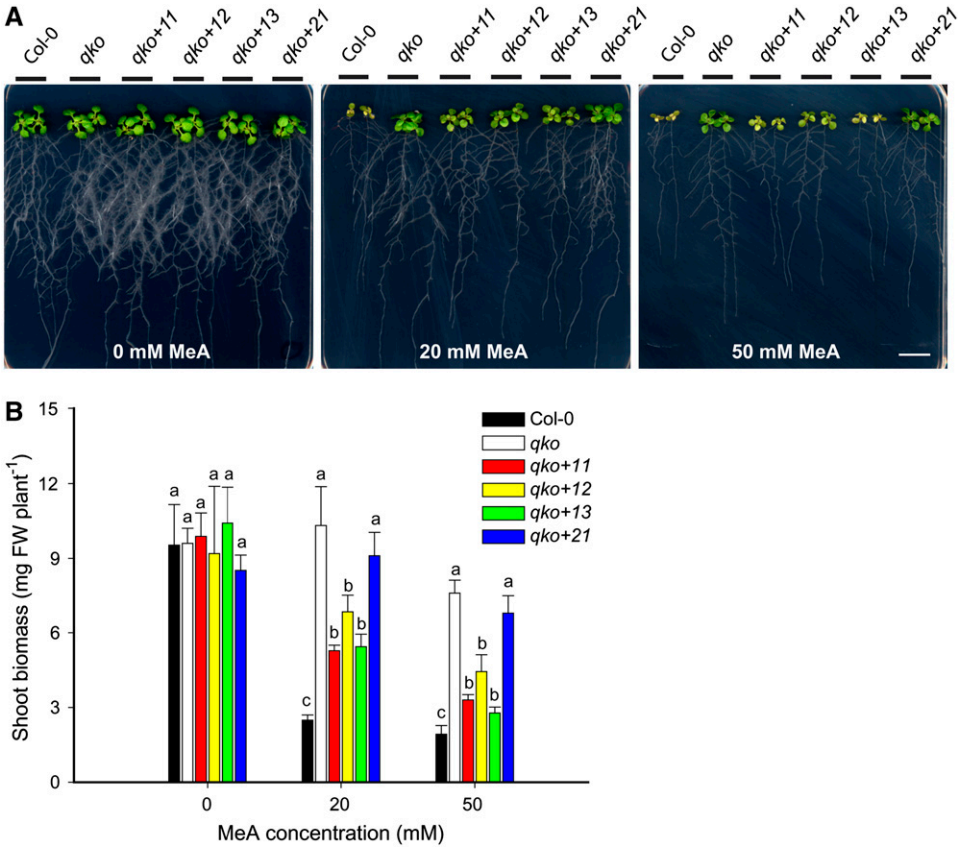

Figure 7. Growth of the Quadruple (*qko*) and Triple Insertion Lines on Increasing Concentrations of MeA.

(A) Growth of the wild type (Col-0), the quadruple insertion line *qko*, and triple insertion lines expressing *AMT1;1* (*qko*+*11*), *AMT1;2* (*qko*+*12*), *AMT1;3* (*qko*+*13*), or *AMT2;1* (*qko*+*21*) on agar containing 0, 20, or 50 mM MeA in the presence 1 mM nitrate and 1% sucrose for 12 d after preculture on half-strength Murashige and Skoog (MS) medium (containing 5 mM nitrate as sole nitrogen source) for 7 d. Bar = 1 cm.

(B) Shoot fresh weights (FW) of the same plants as in **(A)**. Bars indicate means ± SD ($n = 4$), and significant differences at $P < 0.001$ within each group are indicated by different letters.

genes was detected in nitrogen-sufficient roots (Figure 10B). However, *AMT1;5* transcripts accumulated considerably in roots of wild-type plants grown under nitrogen-insufficient conditions (Figure 10B, bottom panel). Interestingly, *AMT1;5* transcript accumulation was highest in the *qko* and *qko*+*21* lines (Figure 10B, bottom panel), suggesting the existence of a possible compensatory upregulation of this homolog in the absence of other AMT genes. However, in a time-course study of plants after they were moved to nitrogen-deficient conditions, *AMT1;5* transcript accumulated in roots earlier in the *qko* line than the wild type, but at later time points, *AMT1;5* transcript levels reached the same levels in both genotypes (see Supplemental Figure 6 online). This pointed to an earlier onset of nitrogen deficiency and thus of *AMT1;5* upregulation in *qko* plants, rather than to a compensatory upregulation in direct response to the absence of other functional *AMT* genes. Root mRNA levels of *AMT1;4* were much lower than those of *AMT1;5*, and in contrast with *AMT1;5*, nitrogen-deficient conditions resulted in little or no increase in *AMT1;4* transcript abundance (Figure 10B, top panel). Thus, AMT1;5 appeared to be the only AMT-type protein that could be responsible for the remaining nitrogen-dependent high-affinity ammonium influx observed in *qko* (Figure 10A).

Characterization of *AMT1;5*

No *Arabidopsis* line with a transposon or T-DNA insertion in *AMT1;5* was available from public *Arabidopsis* seed collections, preventing a functional analysis of the endogenous gene in planta. We therefore took other approaches to address whether *AMT1;5* encodes a functional ammonium transporter. Due to the genetic linkage between *AMT1;5* (At3g24290) and *AMT1;3* (At3g24300) and the Wassilewskija (Ws) ecotype origin of the *amt1;3-1* insertion line, two *AMT1;5* ORFs from the *qko* and Col-0 lines were PCR amplified and cloned independently. Sequence comparison showed only one nucleotide change that generated an Arg-to-Thr substitution at position 9 in the encoded protein from Ws. Functionality of both protein variants was confirmed by their ability to restore growth of the ammonium uptake-defective yeast cells when subjected to low external ammonium concentration as a sole nitrogen source. Cells transformed with

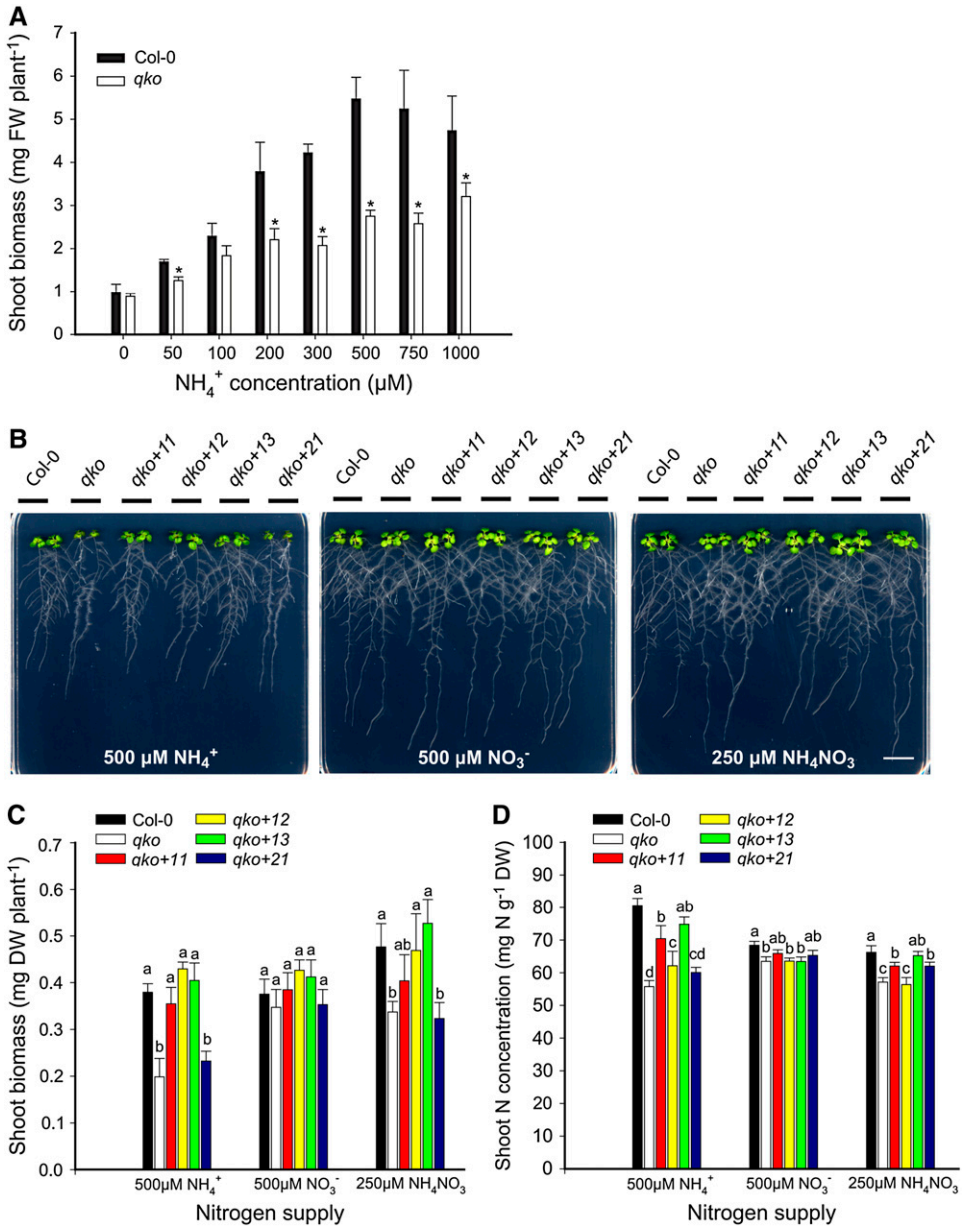

Figure 8. Growth of the Quadruple Insertion Line (*qko*) and Triple Insertion Lines on Different Nitrogen Sources.

(A) Shoot fresh weights (FW) of the wild type (Col-0) and the quadruple insertion line *qko* after growth for 12 d on agar containing different concentrations (from 0 to 1000 μM) of ammonium (supplied as ammonium succinate) and preculture on half-strength MS medium (containing 5 mM nitrate as sole nitrogen source) for 7 d. Bars indicated means ± SD ($n = 4$), and significant differences at $P < 0.001$ are indicated by an asterisk.
(B) Growth of the wild type (Col-0), the quadruple insertion line *qko*, and triple insertion lines expressing *AMT1;1* (*qko+11*), *AMT1;2* (*qko+12*), *AMT1;3* (*qko+13*), or *AMT2;1* (*qko+21*) on agar containing 500 μM NH_4^+ (250 μM as ammonium succinate), 500 μM NO_3^- (500 μM as potassium nitrate), or 250 μM NH_4NO_3 (250 μM ammonium nitrate) for 10 d after preculture on half-strength MS medium (containing 5 mM nitrate as sole N source) for 7 d. Bar = 1 cm.
(C) and **(D)** Shoot dry weights (DW) **(C)** and total shoot nitrogen concentrations **(D)** of the same plants as in **(B)**. Bars indicate means ± SD ($n = 6$), and significant differences at $P < 0.001$ within each group are indicated by different letters.

the empty vector did not restore growth (Figure 11A). Relative to cells expressing *AMT1;3*, however, growth complementation of those expressing *AMT1;5* was weaker, suggesting that *AMT1;5* conferred a smaller ammonium transport capacity to this yeast strain.

We then localized *AMT1;5* promoter activity using transgenic *Arabidopsis* plants expressing a GFP reporter gene driven by the native *AMT1;5* promoter. In roots of plants grown under nitrogen-deficient conditions, GFP-dependent fluorescence was high at the root tip and in the root hair zone where it localized to rhizodermal

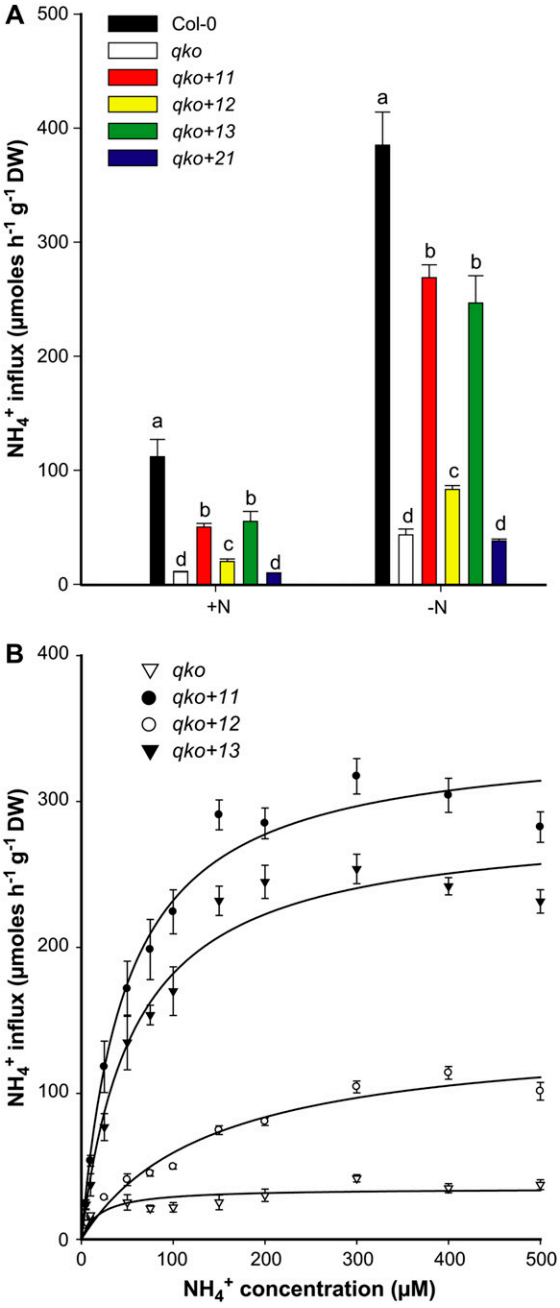

Figure 9. Ammonium Influx Analysis in Roots of the Quadruple (*qko*) and Triple Insertion Lines.

(A) Influx of ^{15}N-labeled ammonium into roots of the wild type (Col-0), the quadruple insertion line *qko*, and triple insertion lines expressing *AMT1;1* (*qko*+*11*), *AMT1;2* (*qko*+*12*), *AMT1;3* (*qko*+*13*), or *AMT2;1* (*qko*+*21*). ^{15}N-labeled ammonium was supplied at a concentration of 200 μM. Bars indicate means ± SD (n = 8 to 10 plants), and significant differences at $P < 0.001$ within each group are indicated by different letters.

(B) Concentration-dependent ^{15}N-labeled ammonium influx into nitrogen-deficient roots (−N) of the quadruple and triple insertion lines. Bars indicate means ± SD (n = 8 to 10 plants). Six-week-old plants were precultured hydroponically under continuous supply of 2 mM ammonium nitrate (+N) or under nitrogen deficiency for 4 d (−N).

cells, including root hairs (Figure 11B). The nitrogen-dependent expression of *AMT1;5* in outer root cells and the ammonium transport activity of AMT1;5 demonstrated in yeast support the notion that AMT1;5 contributes to overall ammonium uptake capacity of nitrogen-deficient *Arabidopsis* roots.

DISCUSSION

In most plant species, ammonium transporters belong to the AMT1- and AMT2/MEP-type classes of proteins and are encoded by gene families (Ludewig et al., 2001). Of the sequenced plant genomes, *Arabidopsis* contains six homologs, *Chlamydomonas* has eight, rice (*Oryza sativa*) has 10, and poplar (*Populus* spp) has 14 (Sonoda et al., 2003; Suenaga et al., 2003; Gonzalez-Ballester et al., 2004; Loqué and von Wirén, 2004; Couturier et al., 2007). How AMT genes might contribute to adaptation of plant species to particular growth conditions and how the number and properties of individual AMT homologs are arranged to achieve productive transport remain important unsolved questions. With the growing knowledge of individual AMT transporters from *Arabidopsis*, this multigene family may serve as a model for how other membrane transporter families are coordinated to achieve controlled substrate transport within plants. Here, we show that biochemical transport properties and the root tissue–specific expression patterns of AMT transporters are important factors that allow them to coordinate effective high-affinity ammonium uptake in *Arabidopsis* roots.

Of the six *Arabidopsis* AMT genes, *AMT1;1*, *AMT1;2*, *AMT1;3*, and *AMT2;1* generally show a high mRNA abundance in roots (Gazzarrini et al., 1999; Birnbaum et al., 2003; Schmid et al., 2005). All four genes are transcriptionally upregulated in roots under nitrogen deficiency or sucrose supply, encode transport proteins that localize to the plasma membrane in planta, and can confer ammonium uptake in yeast and in planta (Gazzarrini et al., 1999; Lejay et al., 2003; Loqué et al., 2006; Engineer and Kranz, 2007; Figures 3, 8, and 9). Ammonium influx studies in single insertion lines indicated that AMT1;1 and AMT1;3 confer with 30 to 35% nearly the same capacity for ammonium uptake in nitrogen-deficient roots (Loqué et al., 2006), while AMT1;2 confers a lower capacity of 18 to 26% (Figure 2). Since the additive contribution of AMT1;1 and AMT1;3 to ammonium uptake in nitrogen-deficient roots accounts for 65 to 70% of the total uptake capacity (Loqué et al., 2006), AMT1;1, AMT1;2, and AMT1;3 together might explain ~90% of the overall ammonium uptake capacity in *Arabidopsis* roots. Transgenic lines in which the root-expressed *AMT2;1* gene was targeted for silencing by RNAi did not reveal a contribution of this transporter to ammonium uptake by roots (Sohlenkamp et al., 2002). Therefore, one may expect the quadruple knockout (*qko*) of all four genes to have ~10% uptake capacity under nitrogen-deficient conditions. This expectation was closely matched by the observation of ammonium influx in *qko* (Figure 9A), showing that >90% of the high-affinity ammonium uptake in *Arabidopsis* roots is conferred by the individual capacities of AMT1;1, AMT1;2, and AMT1;3 working together in an additive manner. Interestingly, each of the three AMT1 capacities was enhanced when plants were shifted from nitrogen-sufficient to -deficient growth conditions (Figure 9A), most probably due to an increased protein synthesis, except

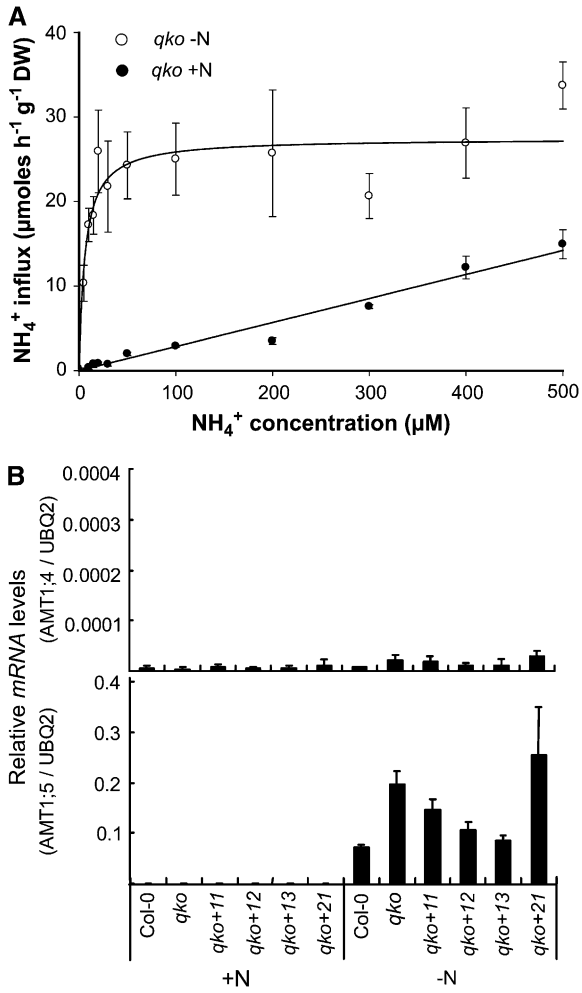

Figure 10. Nitrogen-Dependent Ammonium Influx and *AMT* Gene Expression in Roots of the Quadruple Insertion Line (*qko*).

(A) Concentration-dependent influx of ^{15}N-labeled ammonium into nitrogen-sufficient (+N) or nitrogen-deficient roots (−N) of the quadruple insertion line *qko*. Bars indicate means ± SD ($n = 5$ to 6 plants).

(B) *AMT1;4* and *AMT1;5* mRNA abundance in roots of wild-type or triple insertion lines quantified by real-time RT-PCR relative to the constitutively expressed polyubiquitin control gene (*UBQ2*). Bars indicate means ± SD ($n = 3$). Six week-old plants were precultured hydroponically under continuous supply of 2 mM ammonium nitrate (+N) or under nitrogen deficiency for 4 d (−N).

for AMT1;2 (Figures 1D, 2, and 6). Even though AMT1;2-mediated transport capacity increased under nitrogen deficiency (Figures 2A and 9A), AMT1;2 protein levels remained unchanged (Figures 2C and 2D), suggesting that posttranslational activation may have increased transport capacity (Neuhäuser et al., 2007). Taken together, the three *AMT* genes differ in the inherent transport capacities they encode and in the magnitude of their modulation in response to the nitrogen nutritional status of the plant.

In vivo transport capacities of AMT1;1, AMT1;2, and AMT1;3 as determined in single insertion lines were not exactly the same as those determined using the triple insertion lines. The transport capacity of AMT1;2 (Figure 2) tended to be only slightly higher when comparing single insertion lines with the wild type than *qko+12* with *qko* (Figure 9). By contrast, AMT1;1 and AMT1;3 contributed to 30 to 35% of the wild-type capacity in single insertion lines (Loqué et al., 2006), but this value increased to 55 to 60% when assayed in the corresponding triple insertion lines (Figure 9). Different *Arabidopsis* ecotypes were used as the

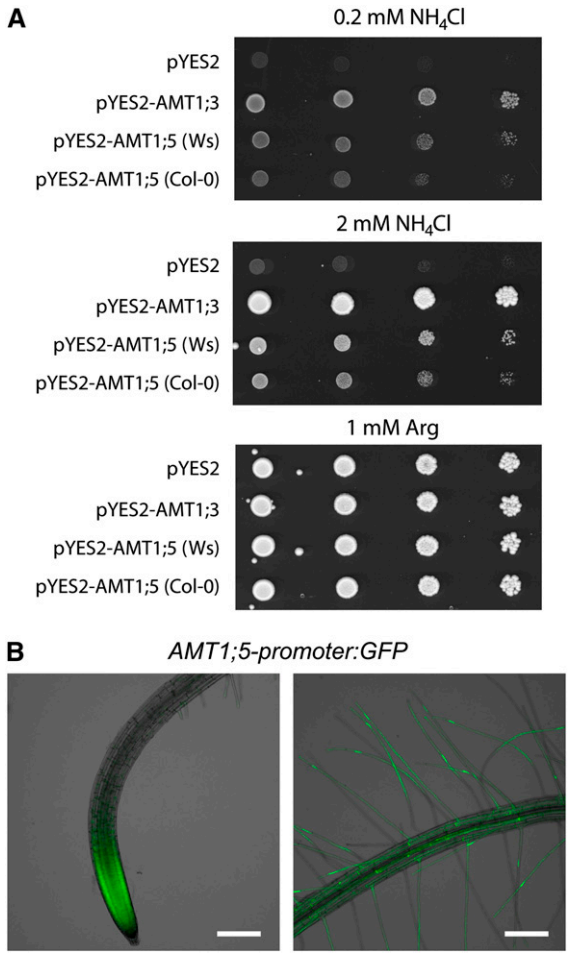

Figure 11. Functional Analysis in Yeast and Localization in Roots of *AMT1;5*.

(A) The triple *mep* yeast mutant (31019b) was transformed with the vectors pYES2, pYES2-AMT1;3, pYES2-AMT1;5 (Ws), or pYES2-AMT1;5 (Col-0). Transformants were selected on YNB medium supplemented with 1 mM Arg. Five microliters of precultured yeast cell suspensions were spotted at onefold to fourfold dilutions on YNB medium supplemented with 2% galactose and either 0.2 or 2 mM NH_4Cl or 1 mM Arg at pH 5.2. Cells were grown at 28°C for 6 d.

(B) Transgenic plants expressing an *AMT1;5-promoter:GFP* fusion construct were grown on agar plates supplemented with 2 mM ammonium nitrate for 2 weeks before being transferred to new media deprived of nitrogen and grown for 5 d. Whole-mount images from root tips and root hair zones were taken by confocal laser scanning microscopy. Bars = 200 μm.

source of mutant alleles in this study. Despite our effort to make the background of the triple insertion lines relatively homogeneous, it cannot be completely excluded that these lines may have differed for other genes influencing the traits being examined. However, segregation of other genes affecting ammonium uptake seems an unlikely explanation for the higher capacities conferred by AMT1;1 and AMT1;3 in the *qko* background relative to the wild type because ammonium uptake capacities of nitrogen-deficient wild-type Col-0, Col-gl, or Ws plants did not differ significantly (Loqué et al., 2006; Figure 9A; see Supplemental Figure 7 online). Moreover, a compensatory upregulation of mRNA or protein levels in response to the absence of other AMT proteins could also be ruled out to explain the higher capacities of AMT1;1 and AMT1;3 shown using the triple insertion lines (Figure 6). A compensatory posttranslational regulation might provide an alternative explanation for these differences. Recently, AMT1;1 was shown to be subjected to a C-terminal phosphorylation modification that inhibits ammonium transport activity (Loqué et al., 2007). Theoretically, a reduction in phosphorylation of AMT1;1 or AMT1;3 in the triple insertion lines expressing these respective proteins might have occurred in response to the absence of other expressed homologs to allow increased transport capacity.

The ammonium influx into nitrogen-sufficient and -deficient *qko* plants indicated the presence of at least another two ammonium uptake systems. A low-capacity transport system with a linear concentration dependency appeared to confer ammonium uptake in nitrogen-sufficient plants (Figure 10A). Its concentration-dependent kinetics was reminiscent of channel-mediated transport and might reflect the activity of NH_3- and/or NH_4^+-conducting aquaporins in the root plasma membrane or of potassium channels, some of which also permeate ammonium (Uozumi et al., 1995; Moroni et al., 1998; Loqué et al., 2005). These or similar transporters could act as low-affinity ammonium transporters, whose contributions extend into the high-affinity range, albeit at a low capacity (Cerezo et al., 2001). In nitrogen-deficient *qko* plants, a second, saturable transport system appeared with a low K_m of ~4.5 μM and a very low capacity that corresponded only to ~5 to 10% of the wild-type transport capacity (Figures 9A and 10A). This transport system might reflect a plant adaptation to very low external ammonium availability, which cannot be efficiently used by AMT1;1 or AMT1;3. In agreement with the study by Engineer and Kranz (2007), quantitative RT-PCR analysis revealed that among the *Arabidopsis* AMT proteins, only AMT1;5 could potentially represent this second saturable transport system, since *AMT1;5* transcripts accumulated under nitrogen deficiency, while *AMT1;4* expression did not respond to nitrogen deficiency and was at least a thousand-fold lower under either nitrogen-deficient or -sufficient conditions (Figure 10B). Moreover, heterologous expression in yeast showed that *AMT1;5* encodes a functional ammonium transporter (Figure 11A), which also suggested AMT1;5 may localize at the plasma membrane in *Arabidopsis*. In addition, promoter activity of *AMT1;5* was observed in the rhizodermis and the root hairs (Figure 11B). These observations support a role for AMT1;5 in accessing external ammonium by uptake across the plasma membrane of rhizodermis cells (Figure 12). Nevertheless, these observations provide only correlative evidence that the residual nitrogen-dependent high-affinity ammonium uptake in the *qko* line depends on

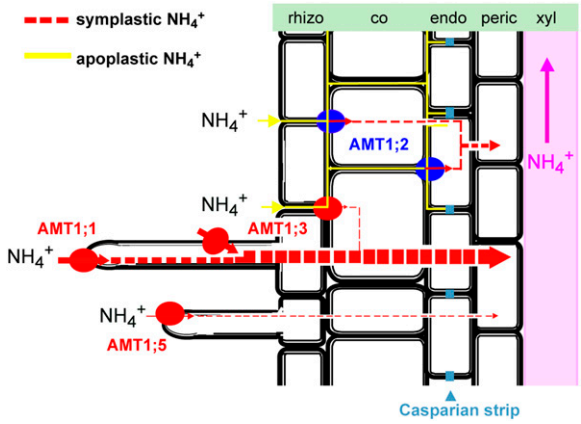

Figure 12. Model Summarizing the Functions of AMT1-Type Transporters in High-Affinity Ammonium Uptake in *Arabidopsis* Roots.

Schematic representation of the contribution to ammonium uptake and spatial expression in root tissues of AMT1;1, AMT1;3, AMT1;5 (all in red), and AMT1;2 (blue) under nitrogen deficiency. AMT-dependent ammonium influx is proportionally represented by the size of their arrows. Ammonium can enter the symplastic route (dashed red line) for radial transport toward the root stele via AMT1;1, AMT1;3, and AMT1;5, which are localized at the plasma membrane of rhizodermis cells, including root hairs. Ammonium can also bypass outer root cells via the apoplastic transport route (yellow line) and subsequently enter the root symplast by AMT1;2-mediated transport across the plasma membrane of endodermal (in the root hair zone) and cortical (in more basal root zones) cells. In the symplast, ammonium can either be assimilated into amino acids or loaded into the xylem by an as yet unidentified transport process. rhizo, rhizodermis; co, cortex; endo, endodermis; peric, pericycle; xyl, xylem.

AMT1;5. Definitive proof would probably require RNAi-mediated silencing of *AMT1;5* in the *qko* background or ethyl methanesulfonate mutagenesis in *qko* followed by a tilling approach to isolate *amt1;5* mutant alleles, since T-DNA or transposon insertion mutants for this gene are not yet available. Nonetheless, the use of T-DNA or transposon insertion mutants for this gene in the generation of a multiple insertion line will be difficult due to the close genetic linkage between *AMT1;5* and *AMT1;3*, and physiological studies will be hampered by the low transport capacity of AMT1;5.

Although AMT2;1 conferred high-affinity ammonium transport in yeast and localized to the plasma membrane (Sohlenkamp et al., 2000, 2002), AMT2;1 did not contribute to overall ammonium uptake in planta. Relative to the *qko* line, the *qko+21* triple insertion line showed neither improved ammonium-dependent growth (Figure 8) nor higher ammonium influx (Figure 9). This observation is consistent with the previous failure to obtain a nitrogen-dependent growth phenotype by RNAi-mediated silencing of *Arabidopsis AMT2;1* (Sohlenkamp et al., 2002). Moreover, AMT2;1 showed a high promoter activity in the root vasculature and a relatively weak activity in cortical cells near the root apex (Sohlenkamp et al., 2002). This particular expression pattern, together with the fact that AMT2;1 belongs to the AMT2 subfamily with potentially different biochemical transport properties to AMT1 transporters (Mayer et al., 2006), raises the possibility that AMT2;1 performs a role in a process other than ammonium acquisition from the rhizosphere. The *qko* and *qko+21* lines

generated in this study should provide a solid basis for future, more extended physiological analyses to uncover the role of AMT2;1.

The triple insertion lines also allowed estimation of substrate affinities of AMT transporters in planta (Figure 9B). AMT1;1 and AMT1;3 showed a very similar affinity for ammonium with K_m values of 50.0 and 60.5 μM, respectively. Considering that ammonium concentrations in soil solutions rarely exceed 50 μM (Marschner, 1995), these K_m values appear to suit their location in rhizodermis cells and root hairs (Figure 12). By contrast, AMT1;2 showed a significantly lower substrate affinity (K_m = 233.9 μM), suggesting adaptation to higher substrate concentrations. AMT1;2 is expressed in endodermal and cortical cells (Figure 4; Neuhäuser et al., 2007), where it resides in the plasma membrane (Figure 3). A location in inner root cells means that substrate for AMT1;2 must come from ammonium that has first been transported radially from the soil through the apoplast in the outer cell layers (Figure 12). To obtain an estimate of the ammonium concentrations that AMT1;2 is facing, we measured ammonium concentrations in apoplastic washing fluid extracted from the roots of wild-type and *amt1;2-1* plants (Figure 5). Interestingly, apoplastic ammonium concentrations in nitrogen-deficient or ammonium-resupplied roots were much higher than those present in the externally supplied solution. This is explained by the Casparian strip forming an apoplastic barrier, which favors a local accumulation of ammonium in the endodermal apoplast (Marschner, 1995). Moreover, continuous efflux of ammonium from cells may help contribute to the millimolar ammonium concentrations found in the apoplast of inner root tissues (Feng et al., 1994; Britto et al., 2001). Indeed, after extraction of ammonium by infiltration of leaf tissue with buffered solutions, apoplastic ammonium concentrations quickly recover and equilibrate in the lower millimolar concentration range (Husted and Schjoerring, 1995; Nielsen and Schjoerring, 1998; Mattsson and Schjoerring, 2002). This buffering capacity will most likely have increased ammonium concentrations in the microenvironment of AMT1;2 above the level supplied in our uptake studies. As a consequence, the determined K_m of 234 μM (Figure 9B) represents an in vivo affinity constant, likely being higher than when assayed under situations in which AMT1;2 directly faces the uptake solution. Indeed, when heterologously expressed in oocytes, AMT1;2 exhibited a K_m value of ~140 μM (Neuhäuser et al., 2007), which is nevertheless more than 10 times higher as that for AMT1;1 determined under the same conditions (Mayer and Ludewig, 2006; Wood et al., 2006). Taken together, AMT1;2 obviously faces higher ammonium concentrations than the AMT1;1 and AMT1;3 rhizodermis-located proteins. The lower K_m of AMT1;2 is therefore suited to this environment, enabling efficient substrate transport close to saturation of the transporter. We therefore conclude that the biochemical transport properties and specific location of AMT1;2 represent an adaptation to retrieval of ammonium that is released from the cortex and that enters the root tissue via the apoplastic transport route.

The findings of this study highlight two principles governing high-affinity ammonium uptake into *Arabidopsis* roots via multiple AMT1-type transport proteins. First, there is a spatial organization of AMT1 transporters, with those transporters possessing higher substrate affinities being located in outer root cells and those of lower affinity being located at the end of the apoplastic transport pathway. At the surface and root hairs of the rhizodermis, ammonium can be directly taken up from the soil solution by AMT1;1, AMT1;3, and AMT1;5 (Figure 12), allowing an immediate transfer into the root symplast for ammonium assimilation by the rhizodermis-localized cytosolic Gln synthetase (Ishiyama et al., 2004). Unassimilated ammonium might be stored in vacuoles (Miller et al., 2001) or further transported symplastically into the root stele, either for assimilation or loading into the xylem where it may accumulate in millimolar concentrations (see Supplemental Figure 3 online). Ammonium that enters the root via the apoplastic route may enter the root symplast through AMT1;2 at the endodermis (Figures 4 and 12). The endodermal expression pattern of AMT1;2 seems to be confined to the root hair zone, which constitutes ~70% of the total root surface (Marschner, 1995). Further up the root, *AMT1;1*, *AMT1;2*, and *AMT1;3* expression extends to cortical cells (Loqué et al., 2006; Figure 4), which provide a large inner surface area for nutrient uptake. This spatial shift might be due to the limited life span of rhizodermis and root hair cells, whose physiological activities usually decrease within a few days (Fusseder, 1987; Neumann et al., 1999). An extension also of AMT1;2 expression to cortex cells in upper root zones might reflect a higher requirement for ammonium retrieval, considering that ammonia-releasing nitrogen catabolism probably increases in older root cells. The second principal highlighted by this study is that high-affinity ammonium transport in *Arabidopsis* roots is conferred by at least four transporters whose capacities likely decrease in the following order: AMT1;1 = AMT1;3 > AMT1;2 > AMT1;5. Although individual ammonium transport capacities, in particular those of AMT1;1 and AMT1;3, might depend on the presence of other transporters, ammonium transport capacities of all four AMT1 proteins increased under nitrogen deficiency (Figure 9; Loqué et al., 2006). To meet the plant's nitrogen demand, it appears that its nutritional status determines the overall ammonium transport capacity, which in turn is broken down into individually modulated AMT1 capacities. Such a coordinated regulation could be brought about by a common regulator, for example, a transcription factor and/or a posttranslational modulator, which is subject to control by the nitrogen demand of the plant. However, nitrogen-sensing proteins or *cis*-acting elements that govern nitrogen demand–regulated expression of genes and proteins involved in nitrogen transport or assimilation still await to be uncovered.

METHODS

Isolation of Transposon Insertion Lines in *AMT1;2* and Generation of Multiple Insertion Lines

The *amt1;2-1* and *amt1;2-2* insertion lines were isolated from the *Arabidopsis thaliana* transposon-tagged (*dSpm*) mutant collection (NASC). Insertions in tagged lines were identified by PCR using the transposon-specific Spm31 primer (5′-GCTTGTTGAACCGACACTTTAACATAAG-3′) and the *AMT1;2* gene-specific primers FKOamt12 (5′-CTTACTACCTCTTCGGATTCGCATTC-3′) and R3KOamt12 (5′-GTTAACAGTTCCACACTATCTGTCC-3′). The *amt2;1-1* line was isolated from the enhancer trap collection of Thomas Jack (Fartmouth College, NH) using as T-DNA–specific primer LB-KOamt21-1 (5′-TCGCCTATAAATACGACGGATCG-3′) and as *AMT2;1* gene-specific primers F1KOamt21-1 (5′-ATGGCCGGAGCTTACGATCCAAGC-3′) and R2KOamt21-1 (5′-AGTGACGCCGGCTAAGCCAGTAACC-3′).

The location of the transposons in the insertion lines was confirmed by sequencing.

The *amt1;1-1* mutant (in Col-gl) and *amt1;3-1* mutant (in Ws) were crossed to give the double insertion line (*dko*) *amt1;1-1 amt1;3-1* (Loqué et al., 2006). A triple insertion line (*tko*) was obtained by crossing the *dko* with *amt2;1-1* (in Col-gl). The F1 plants were backcrossed to the *dko* and selfed. A homozygous *tko* line (*amt1;1-1 amt1;3-1 amt2;1-1*) isolated by PCR was used to generate a quadruple insertion line by crossing *tko* with *amt1;2-1* (in Col-0). After backcrossing to *tko* and selfing, a homozygous *amt1;1-1 amt1;3-1 amt2;1-1 amt1;2-1* line was isolated by PCR. Then, the quadrouple insertion line was backcrossed to wild-type Col-0 and selfed to obtain F2 and F3 populations. Within the F3 population, homozygous lines expressing only one of the four AMT genes were selected by PCR and assigned as *qko+11* (*qko+AMT1;1*), *qko+12* (*qko+AMT1;2*), *qko+13* (*qko+AMT1;3*), and *qko+21* (*qko+AMT2;1*). A homozygous *amt1;1-1 amt1;3-1 amt2;1-1 amt1;2-1* line (*qko*) that served as a reference line was also selected from this population. All lines were then selfed once (F4 generation) before using in phenotypic or physiological analyses.

Plant Culture

Arabidopsis seeds were germinated in the dark for 4 d and precultured on rock wool moistened with tap water. After 1 week, tap water was substituted for nutrient solution containing 1 mM KH_2PO_4, 1 mM $MgSO_4$, 250 μM K_2SO_4, 250 μM $CaCl_2$, 100 μM Na-Fe-EDTA, 50 μM KCl, 50 μM H_3BO_3, 5 μM $MnSO_4$, 1 μM $ZnSO_4$, 1 μM $CuSO_4$, and 1 μM $NaMoO_4$ (pH adjusted to 6.0 by KOH). Unless indicated otherwise, 2 mM NH_4NO_3 was supplied to provide nitrogen-sufficient conditions. The nutrient solution was replaced once a week during the first 3 weeks, twice in the 4th week, and every 2 d in the following weeks. Plants were grown hydroponically under nonsterile conditions in a growth cabinet under the following regime: 10/14 h light/dark; light intensity 280 μmol m^{-2} s^{-1}; temperature 22°C/18°C; 70% humidity.

Phenotypical analysis was conducted in a prefertilized peat-based substrate (www.einheitserde.de) in nutrient solution under supply of 2 mM ammonium nitrate and on sterile agar under supply of ammonium, nitrate, or ammonium nitrate at different concentrations. In plate growth tests of insertion lines, *Arabidopsis* seeds were surface sterilized and plated onto half-strength MS medium (containing 5 mM nitrate as sole nitrogen source) solidified with Difco agar. The plants were precultured for 7 d and transferred to vertical plates containing half-strength MS medium supplemented with different nitrogen sources at indicated concentrations. Plants were grown under axenic conditions in a growth chamber under the above-mentioned conditions except that the light intensity was 120 μmol photons m^{-2} s^{-1}.

Collection of Apoplastic Fluid and Xylem Sap

Arabidopsis plants were grown hydroponically for 6 weeks. Apoplastic fluid of the roots was extracted by centrifugation according to the method of Yu et al. (1999) with some modifications: The harvested roots were dried by blotting and fixed into a 15-mL Falcon tube. By centrifugation at 500*g* for 15 min at 4°C, the solution adhering to the root surface was removed. In a subsequent centrifugation step at 1000*g* for 15 min at 4°C, root apoplastic fluid was collected. A negligible symplastic contamination of the apoplasmic washing fluid was verified by measuring the phosphoenol pyruvate carboxylase activity (EC4.1.1.31). Xylem sap was collected by excision of the hypocotyls below the rosette. The first droplet of sap was removed to prevent contamination of damaged cells. Bleeding sap was then collected in a mounted silicon tube during 30 min, and the volume of the samples was determined. The apoplast extracts and xylem sap samples were stabilized with ice-cold 20 mM HCOOH in a 1:1 volume ratio and stored at −20°C. Ammonium concentrations were analyzed by fluorescence spectroscopy at neutral pH as described by Husted et al. (2000).

RNA Gel Blot Analysis

Total RNA was isolated by phenol-guanidine extraction followed by lithium chloride precipitation or was extracted using TRIzol reagent (Invitrogen). RNA (20 μg per lane) was resolved by electrophoresis in MOPS-formaldehyde agarose gels, blotted onto Hybond N^+ nylon membranes (Amersham), and cross-linked to the membrane by incubation at 80°C for 2 h. The ORFs *AMT1;2* and *AMT2;1* and 3′-ends of *AMT1;1*, *AMT1;2*, and *AMT1;3* were used as probes for hybridization to total RNA. Hybridization to random-primed ^{32}P-radiolabeled probes was performed at 42°C in 50% (v/v) formamide, 1% (w/v) sarkosyl, 5× SSC, and 100 μg mL^{-1} yeast tRNA. Membranes were washed at 42°C twice in 2× SSC, 0.1% (w/v) SDS for 20 min, once in 0.2× SSC, 0.1% (w/v) SDS, and finally in 0.1× SSC, 0.1% (w/v) SDS for 20 min. Ethidium bromide staining of gels was used to monitor evenness of RNA loading.

Isolation of Microsomal Membrane and Plasma Membrane Fractions

Arabidopsis root and shoot tissues were frozen in liquid nitrogen and ground in a mortar. The powder was homogenized in a buffer containing 250 mM Tris-HCl, pH 8.5, 290 mM sucrose, 25 mM EDTA, 5 mM β-mercaptoethanol, 2 mM DTT, and 1 mM phenylmethylsulfonyl fluoride (PMSF). Homogenates were centrifuged at 10,000*g* for 15 min. Supernatants were filtered through nylon mesh (58 μM) and centrifuged at 100,000*g* for 30 min to pellet microsomal membrane fractions. The drained pellet was resuspended in conservation buffer (5 mM bis-Tris-propane, MES, pH 6.5, 250 mM sorbitol, 20% [w/v] glycerol, 1 mM DTT, and 2 mM PMSF) and gently homogenized in a potter.

Plasma membranes were isolated by aqueous two-phase partitioning as described by Larsson et al. (1987). The drained pellet obtained from the above procedure was resuspended in microsomal buffer (5 mM KH_2PO_4, pH 7.8, 330 mM sucrose, and 3 mM KCl) and added to a 36-g phase partitioning system (final concentration: 6.4% dextran T-500, 6.4% polyethylene glycol 3350, 5 mM KH_2PO_4, 3 mM KCl, and 330 mM sucrose). The two phases were mixed and centrifuged at 1500*g* for 5 min. Upper and lower phases were collected separately and repartitioned twice with fresh buffer. The purified phases were diluted with washing buffer and centrifuged at 100,000*g* for 60 min to pellet the membranes. The drained pellets were resuspended in conservation buffer and gently homogenized in a potter. All steps were performed at 4°C. Protein concentrations were determined using a Bradford protein assay (Bio-Rad) with BSA as a standard.

Protein Gel Blot Analysis

Polyclonal antibodies were raised against peptides representing the C terminus of AMT1;2 (n-PWGHFAGRVEPTSRS-c) (Biotrend). The antibodies were affinity purified from serum using a nitrocellulose membrane binding the corresponding peptide as described by Ludewig et al. (2003). Proteins (5 to 10 μg per lane) were denatured in loading buffer (62.5 mM Tris-HCl, pH 6.8, 10% [v/v] glycerol, 2% [w/v] SDS, 2.5% [v/v] β-mercaptoethanol, 0.01% [w/v] bromphenol blue, and 1% PMSF) at 37°C for 30 min or 50°C for 5 min, separated on 10% SDS polyacrylamide gels, and transferred to a polyvinylidene fluoride membrane (Immobilon-P; Millipore) by electroblotting. Blots were developed using the ECL Advance Western Blotting Detection Kit (Amersham) according to the manufacturer's protocol. Primary antibodies and the secondary antibody (peroxidase-linked anti-rabbit IgG; Amersham) were diluted in blocking solution at the following concentrations and combinations: anti-AMT1;1 at 1:400 with secondary antibody at 1:25,000, anti-AMT1;2 at 1:10,000, anti-AMT1;3 at 1:5000, anti-AMT2;1 at 1:4000, anti-AHA2 at 1:10,000 (DeWitt et al., 1996), anti-VPPase (Takasu et al., 1997) at 1;2000, and anti-DET3 at 1:20,000 (Schumacher et al., 1999) with secondary antibody at 1:10,000. MagicMark Western Standard (Invitrogen) was used as molecular weight

marker. Protein blots of DET3, a subunit of the vacuolar ATPase, were used as a control for equal loading.

Localization of AMT1;2 and AMT1;5 by GFP Fusion

For vector construction, DNA fragments of *AMT* genes were amplified from *Arabidopsis* (ecotype Col-0) genomic DNA by PCR using KOD plus DNA polymerase (Toyobo). All PCR products were cloned into pCR-Blunt II-TOPO (Invitrogen) and fully sequenced to confirm identity and lack of polymerase errors. An *AMT1;2 promoter-ORF* fragment covering the 2849-bp 5′-upstream region together with the 1542-bp ORF was amplified by PCR using the primers AMT1;2-GF (5′-GAAGCTTATCCTTCTGTGGATATACTTACGAATAA-3′) and AMT1;2-GR (5′-TCCCGGGGAACAGTCAAGGTCGGTGTAGGAGTCGA-3′). The underlined sequences indicate *Hin*dIII and *Sma*I sites used for fusion construction. The PCR product was cut out as a *Hin*dIII-*Sma*I–ended fragment and ligated to a *Sma*I-*Not*I fragment of EGFP (Clontech) to create a translational fusion at the C terminus of AMT1;2. This *AMT1;2 promoter-ORF-GFP* fusion cassette and an *Not*I-*Eco*RI–ended fragment of the nopaline synthase terminator (T_{NOS}) from the pTH2 vector (Chiu et al., 1996) was cloned between the *Hin*dIII and *Eco*RI sites of pBI101 (Clontech) to obtain an *AMT1;2 PRO-ORF-GFP-*T_{NOS} fusion construct.

The *AMT1;5* promoter fragment covering the 2115-bp 5′-upstream region in *AMT1;5* was amplified by PCR using the primers AMT1;5-pro-F (5′-GAAGCTTGTGCATATTAGTCGTCAAACTGTATTTA-3′) and AMT1;5-pro-R (5′-GCCATGGGTTTTAGAGACTTGAGAGAGGAACCACA-3′). The underlined sequences indicate *Hin*dIII and *Nco*I sites used for fusion construction. The PCR product was cut out as a *Hin*dIII-*Nco*I–ended fragment and ligated to a *Nco*I-*Not*I–ended fragment of EGFP (Clontech) to create a fusion at the translation initiation site of *AMT1;5*. This *AMT1;5* promoter-GFP fusion cassette and a *Not*I-*Eco*RI–ended T_{NOS} fragment from the pTH2 vector (Chiu et al., 1996) was cloned between the *Hin*dIII and *Eco*RI sites of pBI101 (Clontech) to obtain a *AMT1;5 promoter-GFP-*T_{NOS} fusion construct.

The binary plasmids were transferred to *Agrobacterium tumefaciens* GV3101 (pMP90) by the freeze-thaw method (Höfgen and Willmitzer, 1988). *Arabidopsis* (ecotype Col-0) plants were transformed according to the floral dip method (Clough and Bent, 1998). Transgenic plants were selected on agar media of MS composition supplemented with 1% (w/v) sucrose and 50 mg L^{-1} of kanamycin sulfate. The FV500 laser scanning confocal microscopy system (Olympus) was used for the analysis of *AMT1;2 promoter-ORF-GFP* and *AMT1;5 promoter-GFP* plants. GFP was observed under excitation with a 488-nm Ar laser and detected with a 505- to 525-nm band-pass filter.

Real-Time Quantitative RT-PCR

Total RNA was extracted using TRIzol reagent and treated with DNase I (Invitrogen). Reverse transcription was performed using Omniscript reverse transcriptase (Qiagen) and oligo(dT)$_{12-18}$. SYBR *Premix Ex Taq* (Takara) was used for real-time RT-PCR, and signals were detected using a 7500 Fast Real-Time PCR system (Applied Biosystems). Gene-specific primer pairs were for *AMT1;4* (AMT1;4-1067F, 5′-GGCGTCTCCGGCTAGATCTGAGAAC-3′; AMT1;4-1310R, 5′-CGAGCCCGGGTTAAACCCGTACCATC-3′), *AMT;5* (AMT1;5-1871F, 5′-GCGAGGAATGGATTTAGCAGGTCAT-3′; AMT1;5-1985R, 5′-GGCTGGAGGGTTAGGCGCACGAGGT-3′), and *ubiquitin 2* (*UBQ2*) (UBQ2-144F, 5′-CCAAGATCCAGGACAAAGAAGGA-3′; UBQ2-372R, 5′-TGGAGACGAGCATAACACTTGC-3′). The specificity of individual primer pairs among the *AMT* gene family was determined by checking specific amplification from the corresponding target cDNAs. Transcript abundance was calculated by fitting to standard curves of specific cDNAs.

Heterologous Expression of *AMT1;5* in Yeast

The ORF of *AMT1;5* was amplified by PCR from genomic DNA (*Arabidopsis* Col-0, Ws, and *qko* line) using the specific primers AMT1;5-For (5′-CCCAGGCTTATGTCAGGAGCTATTACTTGCT-3′) and AMT1;5-Rev (5′-CCGCTCGAGTCAAACGGCTGGAGGGTTAGG-3′). The amplified fragment was cloned into the pGEM-T Easy vector (Promega), and DNA sequences were verified. The *Eco*RI fragment was subcloned into the yeast expression vector pYES2 (Invitrogen) resulting in the plasmid, which was used for the transformation of the triple *mep* deletion yeast strain 31019b (Marini et al., 1997). Growth complementation assays were performed on solid YNB medium supplemented with 2% galactose and a nitrogen source (1 mM Arg and 0.2 or 2 mM ammonium chloride) and buffered at pH 5.2 by 50 mM MES-Tris.

Heterologous Expression of the Chimeric *AMT1;2* Protein in Yeast

The ORF of *AMT1;2* was amplified by PCR from reverse-transcribed *Arabidopsis* Col-0 cDNA using KOD$^+$ DNA polymerase (Toyobo) with the specific primers AMT1;2-F (5′-TCCCTCCCTCCCTCTCCACCATGGACAC-3′) and AMT1;2-R (5′-TCAAACAGTCAAGGTCGGTGTAGGAGTC-3′). The amplified DNA fragment was cloned into pCR-BluntII-TOPO (Invitrogen) and sequenced. The cDNA was then digested by *Eco*RI and subcloned into p426 to generate a p426-AMT1;2 plasmid. The 5′-flanking DNA fragment of the transposon, including a part of the transposon in the *atamt1;2-2* insertion line, was amplified by PCR using the transposon-specific Spm31 primer and the *AMT1;2* gene-specific primer FKOamt12 to be cloned into the pGEM-T Easy vector (Promega) and sequenced. The 3′-end of *AMT1;2* in p426 was excised by *Xho*I and substituted by the 3′-end of the *AMT1;2* transposon fusion fragment from the *Xho*I restriction site into the *Sal*I site located in pGEM-T to generate a p426-AMT1;2-2 plasmid. Empty p426, p426-AMT1;2, and p426-AMT1;2-2 plasmids were used for the transformation of the triple *mep* deletion yeast strain 31019b (Marini et al., 1997). Growth complementation assays were performed on solid YNB medium supplemented with 3% glucose and 1, 5, and 10 mM NH_4Cl or 5 mM Arg as the sole nitrogen source.

^{15}N Uptake Analysis

Influx measurements of ^{15}N-labeled NH_4^+ in plant roots were conducted after rinsing the roots in 1 mM $CaSO_4$ solution for 1 min, followed by an incubation for 6 min in nutrient solution containing different concentrations of ^{15}N-labeled NH_4^+ (95 atom% ^{15}N) as a sole nitrogen source, and finally washed in 1 mM $CaSO_4$ solution. Roots were harvested and stored at −70°C before freeze-drying. Each sample was ground, and 1.5 mg was used for ^{15}N determination by isotope ratio mass spectrometry (Finnigan). Values obtained for concentration-dependent ammonium influx up to 500 μM ammonium were directly fitted to the Michaelis-Menten equation.

Accession Numbers

Arabidopsis Genome Initiative locus identifiers for the genes mentioned in this articles are At4g13510 (*AMT1;1*), At1g64780 (*AMT1;2*), At3g24300 (*AMT1;3*), At4g28700 (*AMT1;4*), At3g24290 (*AMT1;5*), and At2g38290 (*AMT2;1*).

Supplemental Data

The following materials are available in the online version of this article.

Supplemental Figure 1. The *AMT1;2-2* Mutant Allele Is Nonfunctional When Heterologously Expressed in Yeast.

Supplemental Figure 2. The Insertion Lines *amt1;2-1* and *amt1;2-2* Show Decreased Methylammonium Sensitivity.

Supplemental Figure 3. The Insertion Lines *amt1;2-1* and *amt1;2-2* Do Not Show Altered Ammonium Concentrations in the Xylem Sap.

Supplemental Figure 4. The *amt2;1* T-DNA Insertion Line.

Supplemental Figure 5. Growth of the Quadruple Insertion Line (*qko*) on Millimolar Ammonium Concentrations.

Supplemental Figure 6. Time-Dependent Accumulation of *AMT1;5* mRNA under Nitrogen Deficiency.

Supplemental Figure 7. Comparison of the Influx of ^{15}N-Labeled Ammonium into Roots of Three *Arabidopsis* Ecotypes.

ACKNOWLEDGMENTS

We thank Elke Dachtler and Susanne Reiner for skillful technical support, Joni Lima, Fanghua Ye, Fugang Ren, Anne Bohner, and Anderson Meda for help with the ammonium influx experiments, and Bernhard Bauer (all University of Hohenheim, Stuttgart, Germany) for help with ammonium measurements. We also thank Doris Rentsch (University of Bern, Switzerland), who kindly provided the AMT2;1 antibody and the *amt2;1-1* insertion line, Karin Schumacher (Center for Plant Molecular Biology, Tuebingen, Germany) for kindly providing the AHA2 and DET3 antibodies, and Masayoshi Maeshima (University of Nagoya, Japan) for the VPPase antibody. We especially thank Nick Collins (ACPFG, Adelaide, Australia) for critically reading the manuscript. This study was supported by a grant from the Deutsche Forschungsgemeinschaft (Bonn, Germany) to N.V.W. (WI1728/4-2) and by Grants-in-Aid for Scientific Research in Priority Areas from the Ministry of Education, Culture, Sports, Science, and Technology of Japan to H.T.

Received April 9, 2007; revised July 13, 2007; accepted July 23, 2007; published August 10, 2007.

REFERENCES

Birnbaum, K., Shasha, D.E., Wang, J.Y., Jung, J.W., Lambert, G.M., Galbraith, D.W., and Benfey, P.N. (2003). A gene expression map of the Arabidopsis root. Science **302:** 1956–1960.

Bloom, A.J., Jackson, L.E., and Smart, D.R. (1993). Root growth as a function of ammonium and nitrate in the root zone. Plant Cell Environ. **16:** 199–206.

Britto, D.T., and Kronzucker, H.J. (2002). NH_4^+ toxicity in higher plants: A critical review. J. Plant Physiol. **159:** 567–584.

Britto, D.T., Siddiqi, M.Y., Glass, A.D., and Kronzucker, H.J. (2001). Futile transmembrane NH_4^+ cycling: A cellular hypothesis to explain ammonium toxicity in plants. Proc. Natl. Acad. Sci. USA **98:** 4255–4258.

Cerezo, M., Tillard, P., Filleur, S., Munos, S., Daniel-Vedele, F., and Gojon, A. (2001). Major alterations of the regulation of root NO_3^- uptake are associated with the mutation of *NRT2.1* and *NRT2.2* genes in Arabidopsis. Plant Physiol. **127:** 262–271.

Chiu, W.L., Niwa, Y., Zeng, W., Hirano, T., Kobayashi, H., and Sheen, J. (1996). Engineered GFP as a vital reporter in plants. Curr. Biol. **6:** 325–330.

Clough, S.J., and Bent, A.F. (1998). Floral dip: A simplified method for *Agrobacterium*-mediated transformation of *Arabidopsis thaliana*. Plant J. **16:** 735–743.

Couturier, J., Montanini, B., Martin, F., Brun, A., Blaudez, D., and Chalot, M. (2007). The expanded family of ammonium transporters in the perennial poplar plant. New Phytol. **174:** 137–150.

DeWitt, N.D., Hong, B.M., Sussman, M.R., and Harper, J.F. (1996). Targeting of two Arabidopsis H^+-ATPase isoforms to the plasma membrane. Plant Physiol. **112:** 833–844.

Engineer, C.B., and Kranz, R.G. (2007). Reciprocal leaf and root expression of AtAmt1.1 and root architectural changes in response to nitrogen starvation. Plant Physiol. **143:** 236–250.

Feng, J., Volk, R.J., and Jackson, W.A. (1994). Inward and outward transport of ammonium in roots of maize and sorghum: Contrasting effects of methionine sulphoximine. J. Exp. Bot. **45:** 429–439.

Finnemann, J., and Schjoerring, J.K. (1999). Translocation of ammonium in oilseed rape plants in relation to glutamine synthase isogen expression and activity. Physiol. Plant **105:** 469–477.

Fusseder, A. (1987). The longevity and activity of the primary root of maize. Plant Soil **101:** 257–265.

Gazzarrini, S., Lejay, L., Gojon, A., Ninnemann, O., Frommer, W.B., and von Wirén, N. (1999). Three functional transporters for constitutive, diurnally regulated, and starvation-induced uptake of ammonium into *Arabidopsis* roots. Plant Cell **11:** 937–947.

Gonzalez-Ballester, D., Camargo, A., and Fernandez, E. (2004). Ammonium transporter genes in Chlamydomonas: The nitrate-specific regulatory gene Nit2 is involved in Amt1;1 expression. Plant Mol. Biol. **56:** 863–878.

Hirner, A., Ladwig, F., Stransky, H., Okumoto, S., Keinath, M., Harms, A., Frommer, W.B., and Koch, W. (2006). Arabidopsis LHT1 is a high-affinity transporter for cellular amino acid uptake in both root epidermis and leaf mesophyll. Plant Cell **18:** 1931–1946.

Hirsch, R.E., Lewis, B.D., Spalding, E.P., and Sussman, M.R. (1998). A role for the AKT1 potassium channel in plant nutrition. Science **280:** 918–921.

Höfgen, R., and Willmitzer, L. (1988). Storage of competent cells for *Agrobacterium* transformation. Nucleic Acids Res. **16:** 9877.

Hussain, D., Haydon, M.J., Wang, Y., Wong, E., Sherson, S.M., Young, J., Camakaris, J., Harper, J.F., and Cobbett, C.S. (2004). P-type ATPase heavy metal transporters with roles in essential zinc homeostasis in *Arabidopsis*. Plant Cell **16:** 1327–1339.

Husted, S., Hebbern, C.A., Mattsson, M., and Schjoerring, J.K. (2000). A critical experimental evaluation of methods for determination of NH_4^+ in plant tissue, xylem sap and apoplastic fluid. Physiol. Plant. **109:** 167–179.

Husted, S., and Schjoerring, J.K. (1995). A computer-controlled system for studying ammonia exchange, photosynthesis and transpiration of plant canopies growing under controlled environmental-conditions. Plant Cell Environ. **18:** 1070–1077.

Ishiyama, K., Inoue, E., Watanabe-Takahashi, A., Obara, M., Yamaya, T., and Takahashi, H. (2004). Kinetic properties and ammonium-dependent regulation of cytosolic isoenzymes of glutamine synthetase in Arabidopsis. J. Biol. Chem. **279:** 16598–16605.

Javelle, A., Thomas, G., Marini, A.M., Kramer, R., and Merrick, M. (2005). In vivo functional characterization of the *Escherichia coli* ammonium channel AmtB: Evidence for metabolic coupling of AmtB to glutamine synthetase. Biochem. J. **390:** 215–222.

Javot, H., Lauvergeat, V., Santoni, V., Martin-Laurent, F., Guclu, J., Vinh, J., Heyes, J., Franck, K.I., Schaffner, A.R., Bouchez, D., and Maurel, C. (2003). Role of a single aquaporin isoform in root water uptake. Plant Cell **15:** 509–522.

Kaiser, B.N., Rawat, S.R., Siddiqi, M.Y., Masle, J., and Glass, A.D. (2002). Functional analysis of an Arabidopsis T-DNA "Knockout" of the high-affinity NH_4^+ transporter AtAMT1;1. Plant Physiol. **130:** 1263–1275.

Kataoka, T., Watanabe-Takahashi, A., Hayashi, N., Ohnishi, M., Mimura, T., Buchner, P., Hawkesford, M.J., Yamaya, T., and Takahashi, H. (2004). Vacuolar sulfate transporters are essential determinants controlling internal distribution of sulfate in *Arabidopsis*. Plant Cell **16:** 2693–2704.

Khademi, S., O'Connell, J., Remis, J., Robles-Colmenares, Y., Miercke, L.J., and Stroud, R.M. (2004). Mechanism of ammonia transport by Amt/MEP/Rh: structure of AmtB at 1.35 A. Science **305:** 1587–1594.

Lanquar, V., Lelievre, F., Bolte, S., Hames, C., Alcon, C., Neumann, D., Vansuyt, G., Curie, C., Schroder, A., Kramer, U., Barbier-Brygoo, H., and Thomine, S. (2005). Mobilization of vacuolar iron by AtNRAMP3 and AtNRAMP4 is essential for seed germination on low iron. EMBO J. **24:** 4041–4051.

Larsson, C., Widell, S., and Kjellbom, P. (1987). Preparation of high-purity plasma membranes. Methods Enzymol. **148:** 558–568.

Lejay, L., Gansel, X., Cerezo, M., Tillard, P., Muller, C., Krapp, A., von Wirén, N., Daniel-Vedele, F., and Gojon, A. (2003). Regulation of root ion transporters by photosynthesis: Functional importance and relation with hexokinase. Plant Cell **15:** 2218–2232.

Loqué, D., Lalonde, S., Looger, L.L., von Wirén, N., and Frommer, W.B. (2007). A cytosolic trans-activation domain essential for ammonium uptake. Nature **446:** 195–198.

Loqué, D., Ludewig, U., Yuan, L., and von Wirén, N. (2005). Tonoplast intrinsic proteins AtTIP2;1 and AtTIP2;3 facilitate NH_3 transport into the vacuole. Plant Physiol. **137:** 671–680.

Loqué, D., and von Wirén, N. (2004). Regulatory levels for the transport of ammonium in plant roots. J. Exp. Bot. **55:** 1293–1305.

Loqué, D., Yuan, L., Kojima, S., Gojon, A., Wirth, J., Gazzarrini, S., Ishiyama, K., Takahashi, H., and von Wirén, N. (2006). Additive contribution of AMT1;1 and AMT1;3 to high-affinity ammonium uptake across the plasma membrane of nitrogen-deficient Arabidopsis roots. Plant J. **48:** 522–534.

Ludewig, U. (2006). Ion transport versus gas conduction: Function of AMT/Rh-type proteins. Transfus. Clin. Biol. **13:** 111–116.

Ludewig, U., von Wirén, N., Rentsch, D., and Frommer, W.B. (2001). Rhesus factors and ammonium: A function in efflux? Genome Biol. **2:** 1010.1–1010.5.

Ludewig, U., Wilken, S., Wu, B., Jost, W., Obrdlik, P., El Bakkoury, M., Marini, A.M., Andre, B., Hamacher, T., Boles, E., von Wirén, N., and Frommer, W.B. (2003). Homo- and hetero-oligomerization of ammonium transporter-1 NH_4^+ uniporters. J. Biol. Chem. **278:** 45603–45610.

Marini, A.M., Soussi-Boudekou, S., Vissers, S., and Andre, B. (1997). A family of ammonium transporters in *Saccharomyces cerevisiae*. Mol. Cell. Biol. **17:** 4282–4293.

Marschner, H. (1995). Mineral Nutrition of Higher Plants. (London: Academic Press).

Mattsson, M., and Schjoerring, J.K. (2002). Dynamic and steady-state responses of inorganic nitrogen pools and NH_3 exchange in leaves of *Lolium perenne* and *Bromus erectus* to changes in root nitrogen supply. Plant Physiol. **128:** 742–750.

Mayer, M., and Ludewig, U. (2006). Role of AMT1;1 in NH_4^+ acquisition in *Arabidopsis thaliana*. Plant Biol. **8:** 522–528.

Mayer, M., Schaaf, G., Mouro, I., Lopez, C., Colin, Y., Neumann, P., Cartron, J.P., and Ludewig, U. (2006). Different transport mechanisms in plant and human AMT/Rh-type ammonium transporters. J. Gen. Physiol. **127:** 133–144.

Miller, A.J., Cookson, S.J., Smith, S.J., and Wells, D.M. (2001). The use of microelectrodes to investigate compartmentation and the transport of metabolized inorganic ions in plants. J. Exp. Bot. **52:** 541–549.

Moroni, A., Bardella, L., and Thiel, G. (1998). The impermeant ion methylammonium blocks K+ and NH4+ currents through KAT1 channel differently: Evidence for ion interaction in channel permeation. J. Membr. Biol. **163:** 25–35.

Neuhäuser, B., Dynowski, M., Mayer, M., and Ludewig, U. (2007). Regulation of NH_4^+ transport by essential cross talk between AMT monomers through the carboxyl tails. Plant Physiol. **143:** 1651–1659.

Neumann, G., Massonneau, A., Martinoia, E., and Romheld, V. (1999). Physiological adaptations to phosphorus deficiency during proteoid root development in white lupin. Planta **208:** 373–382.

Nielsen, K.H., and Schjoerring, J.K. (1998). Regulation of apoplastic NH_4^+ concentration in leaves of oilseed rape. Plant Physiol. **118:** 1361–1368.

Rahayu, Y.S., Walch-Liu, P., Neumann, G., Romheld, V., von Wirén, N., and Bangerth, F. (2005). Root-derived cytokinins as long-distance signals for NO_3^--induced stimulation of leaf growth. J. Exp. Bot. **56:** 1143–1152.

Rawat, S.R., Silim, S.N., Kronzucker, H.J., Siddiqi, M.Y., and Glass, A.D. (1999). *AtAMT1* gene expression and NH_4^+ uptake in roots of *Arabidopsis thaliana*: evidence for regulation by root glutamine levels. Plant J. **19:** 143–152.

Schmid, M., Davison, T.S., Henz, S.R., Pape, U.J., Demar, M., Vingron, M., Scholkopf, B., Weigel, D., and Lohmann, J.U. (2005). A gene expression map of *Arabidopsis thaliana* development. Nat. Genet. **37:** 501–506.

Schumacher, K., Vafeados, D., McCarthy, M., Sze, H., Wilkins, T., and Chory, J. (1999). The Arabidopsis *det3* mutant reveals a central role for the vacuolar H^+-ATPase in plant growth and development. Genes Dev. **13:** 3259–3270.

Shin, H., Shin, H.S., Dewbre, G.R., and Harrison, M.J. (2004). Phosphate transport in Arabidopsis: Pht1;1 and Pht1;4 play a major role in phosphate acquisition from both low- and high-phosphate environments. Plant J. **39:** 629–642.

Sohlenkamp, C., Shelden, M., Howitt, S., and Udvardi, M. (2000). Characterization of *Arabidopsis* AtAMT2, a novel ammonium transporter in plants. FEBS Lett. **467:** 273–278.

Sohlenkamp, C., Wood, C.C., Roeb, G.W., and Udvardi, M. (2002). Characterization of *Arabidopsis* AtAMT2, a high-affinity ammonium transporter of the plasma membrane. Plant Physiol. **130:** 1788–1796.

Sonoda, Y., Ikeda, A., Saiki, S., von Wirén, N., Yamaya, T., and Yamaguchi, J. (2003). Distinct expression and function of three ammonium transporter genes (OsAMT1;1-1;3) in rice. Plant Cell Physiol. **44:** 726–734.

Suenaga, A., Moriya, K., Sonoda, Y., Ikeda, A., von Wirén, N., Hayakawa, T., Yamaguchi, J., and Yamaya, T. (2003). Constitutive expression of a novel-type ammonium transporter OsAMT2 in rice plants. Plant Cell Physiol. **44:** 206–211.

Takano, J., Wada, M., Ludewig, U., Schaaf, G., von Wirén, N., and Fujiwara, T. (2006). The Arabidopsis major intrinsic protein NIP5;1 is essential for efficient boron uptake and plant development under boron limitation. Plant Cell **18:** 1498–1509.

Takasu, A., Nakanishi, Y., Yamauchi, T., and Maeshima, M. (1997). Analysis of the substrate binding site and carboxyl terminal region of vacuolar H+-pyrophosphatase of mung bean with peptide antibodies. J. Biochem. (Tokyo) **122:** 883–889.

Tissier, A.F., Marillonnet, S., Klimyuk, V., Patel, K., Torres, M.A., Murphy, G., and Jones, J.D.G. (1999). Multiple independent defective suppressor-mutator transposon insertions in Arabidopsis: A tool for functional genomics. Plant Cell **11:** 1841–1852.

Uozumi, N., Gassmann, W., Gao, Y.W., and Schroeder, J.I. (1995). Identificaion of strong modification in cation selectivity in an *Arabidopsis* inward rectifying potassium channel by mutant selection in yeast. J. Biol. Chem. **270:** 24276–24281.

von Wirén, N., and Merrick, M. (2004). Regulation and function of ammonium carriers in bacteria, fungi and plants. In Molecular Mechanisms Controlling Transmembrane Transport, Topics in Current Genetics, Vol. 9, E. Boles and R. Krämer, eds (Heidelberg, Germany: Springer Berlin Press), pp. 95–120.

Walch-Liu, P., Neumann, G., Bangerth, F., and Engels, C. (2000). Rapid effects of nitrogen form on leaf morphogenesis in tobacco. J. Exp. Bot. **51:** 227–237.

Wood, C.C., Poree, F., Dreyer, I., Koehler, G.J., and Udvardi, M.K. (2006). Mechanisms of ammonium transport, accumulation, and retention in ooyctes and yeast cells expressing Arabidopsis AtAMT1;1. FEBS Lett. **580:** 3931–3936.

Yu, Q., Tang, C., Chen, Z., and Kuo, J. (1999). Extraction of apoplastic sap from plant roots by centrifugation. New Phytol. **143:** 299–304.

Yuan, L., Loqué, D., Ye, F., Frommer, W.B., and von Wirén, N. (2007). Nitrogen-dependent posttranscriptional regulation of the ammonium transporter AtAMT1;1. Plant Physiol. **143:** 732–744.

Zheng, L., Kostrewa, D., Berneche, S., Winkler, F.K., and Li, X.D. (2004). The mechanism of ammonia transport based on the crystal structure of AmtB of *Escherichia coli*. Proc. Natl. Acad. Sci. USA **101:** 17090–17095.